

**INTENSITY INVARIANT PATTERN RECOGNITION OF UNSEGMENTED
TARGETS USING NORMALIZED JOINT TRANSFORM CORRELATION**

by

Abul Bashar Mohammad Ishtek Hossain

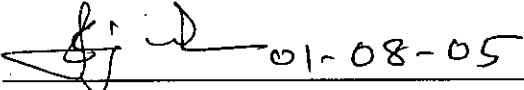
MASTER OF SCIENCE IN ELECTRICAL AND ELECTRONIC ENGINEERING



**DEPARTMENT OF ELECTRICAL AND ELECTRONIC ENGINEERING
BANGLADESH UNIVERSITY OF ENGINEERING AND TECHNOLOGY
2005**

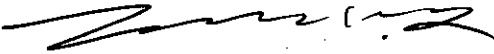
The thesis titled “Intensity invariant pattern recognition of unsegmented targets using normalized joint transform correlation”, submitted by Abul Bashar Mohammad Ishtek Hossain, Roll No. 040306218P, Session April 2003, has been accepted as satisfactory in partial fulfillment of the requirement for the degree of MASTER OF SCIENCE IN ELECTRICAL AND ELECTRONIC ENGINEERING on 01 August 2005.

BOARD OF EXAMINERS

1.  01-08-05

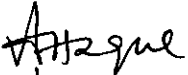
Dr. Satya Prasad Majumder
Professor
Department of Electrical and Electronic Engineering
BUET, Dhaka-1000, Bangladesh

Chairman
(Supervisor)

2.  _____


Dr. S. Shahnawaz Ahmed
Professor and Head
Department of Electrical and Electronic Engineering
BUET, Dhaka-1000, Bangladesh

Member
(Ex-officio)

3.  _____

Dr. Md. Aynal Haque
Professor
Department of Electrical and Electronic Engineering
BUET, Dhaka-1000, Bangladesh

Member

4.  _____

Md. Abdul Moqaddem
Deputy General Manager
Billing Systems, Teletalk Bangladesh Ltd.
H#41, R#27, Block#A, Banani, Dhaka-1213.

Member
(External)

DECLARATION

It is hereby declared that this thesis or any part of it has not been submitted elsewhere for the award of any degree or diploma.

Signature of the Candidate

Ishtek Hossain

Abul Bashar Mohammad Ishtek Hossain

DEDICATION

To my beloved parents.

CONTENTS

LIST OF TABLES	iv
LIST OF FIGURES	vi
LIST OF ABBREVIATIONS	x
LIST OF SYMBOLS	xi
ACKNOWLEDGEMENTS	xii
ABSTRACT	xiii
1. INTRODUCTION	1
1.1 Introduction	1
1.2 Classification of Pattern Recognition tasks	2
1.2.1 Statistical Pattern Recognition	2
1.2.2 Syntactic Pattern Recognition	2
1.2.3 Neural Pattern Recognition	3
1.3 Implementation Techniques of Pattern Recognition	3
1.4 Optical Pattern Recognition	3
1.4.1 VanderLugt Correlator (VLC)	4
1.4.2 Joint Transform Correlator (JTC)	5
1.5 Intensity Invariant Pattern Recognition	8
1.6 Objectives of the Thesis	8
1.7 Thesis Outline	9
2. JOINT TRANSFORM CORRELATION TECHNIQUE	
2.1 Introduction	10
2.2 Classical Joint Transform Correlation Technique	10
2.2.1 Single Target Detection	12
2.2.1.1 Analysis	12
2.2.1.2 Simulation Results	13
2.2.2 Multiple Target Detection	16

2.2.2.1 Analysis	16
2.2.2.2 Simulation Results	17
2.3 Classical Joint Transform Correlation with Image Subtraction	22
2.3.1 Analysis	22
2.3.2 Simulation Results	23
2.4 Fringe-adjusted Joint Transform Correlation with Image Subtraction	25
2.4.1 Analysis	25
2.4.2 Simulation Results	26
2.5 Conclusion	29
3. NORMALIZED JOINT TRANSFORM CORRELATION ALGORITHM	
3.1 Introduction	30
3.2 Unnormalized Intensity Varying Multi-target Detection	30
3.2.1 Theoretical Analysis	30
3.2.1 Simulation Results	32
3.3 Normalized Intensity Varying Multi-target Detection	35
3.3.1 Normalized Correlation	35
3.3.2 Theoretical Analysis	38
3.3.3 Simulation Results	40
3.4 Post Processing Technique	46
3.4.1 Theoretical Analysis	46
3.4.1 Simulation Results	47
3.5 Performance Evaluation of the Proposed Scheme	48
3.5.1 Performance Evaluation	48
3.5.2 Comparative Analysis	51
3.6 Detection of Gray Scale Image	52
3.6.1 Input Scene Containing Only Targets	52
3.6.2 Performance Evaluation	55
3.6.3 Input Scene Containing Targets and Non-Targets	56
3.6.4 Performance Evaluation	59
3.6.5 Comparative Analysis	59
3.7 Detection of Targets Under Noisy Conditions	60

3.7.1 Noisy Binary Image detection	60
3.7.1.1 Binary Image Containing Only Targets	60
3.7.1.2 Performance Evaluation	64
3.7.1.3 Binary Image Containing Targets and Non-Targets	64
3.7.1.4 Performance Evaluation	66
3.7.2 Noisy Gray Level Image detection	67
3.7.2.1 Simulation Results	68
3.7.2.2 Performance Evaluation	70
3.7.2.3 Comparative Analysis	70
3.8 Modified Normalized Correlation	71
3.8.1 Theoretical Analysis	71
3.8.2 Simulation Results	73
3.8.2.1 Binary Image Detection	73
3.8.2.2 Gray Level Image Detection	78
3.8.2.3 Noisy Image Detection	79
3.8.2.4 Comparative Analysis	81
3.9 Conclusion	81
4. CONCLUSIONS	
4.1 Conclusion	83
4.2 Future Works	85
REFERENCES	86

LIST OF TABLES

	Page No.
3.1 Comparative analysis of classical JTC and normalized JTC where the input plane contains only targets	49
3.2 Comparative study of input image containing targets and non-targets.	50
3.3 Applying the post processing technique to the input scene with only targets but illumination varying	50
3.4 Comparative analysis of normalized JTC with the morphological JTC	51
3.5 Performance analysis in the detection of grayscale image lena	55
3.6 Performance analysis in the detection of grayscale image of targets and non-targets	59
3.7 Comparative analysis of normalized JTC with the morphological JTC	59
3.8 Detection performance binary images containing targets only in noisy conditions without post processing.	64
3.9 Detection performance binary images containing targets only in noisy conditions with post processing.	64
3.10 Detection performance binary images containing targets and non targets in noisy conditions without post processing.	66
3.11 Detection performance binary images containing targets and non targets in noisy conditions with post processing.	67
3.12 Detection performance of gray level in noisy conditions without post processing.	69
3.13 Detection performance of binary images in noisy conditions with post processing.	70
3.14 Comparative analysis of normalized JTC with the morphological JTC	70

3.15	Detection performance of binary images consisting of targets and non-targets with post processing.	76
3.16	Detection performance of binary images consisting of targets only with post processing.	77
3.17	Detection performance of gray level images using the modified normalized correlation technique.	78
3.18	Comparative analysis of normalized JTC with the morphological JTC	81

LIST OF FIGURES

	Page No.	
2.1	Classical JTC architecture with Image subtraction	11
2.2 (a)	Input joint image of identical target object	14
2.2 (b)	Classical JTC output of Fig. 2.1 (a)	14
2.3 (a)	Input joint image of non-target object	15
2.3 (b)	Classical JTC output of Fig. 2.3 (a)	15
2.4 (a)	Input joint image with identical targets	18
2.4 (b)	Classical JTC output of Fig. 2.4 (a)	18
2.5 (a)	Input image with two non-targets	19
2.5 (b)	Classical JTC output of Fig. 2.5 (a)	19
2.6 (a)	Input joint image with one target and one non-target	20
2.6 (b)	Classical JTC output of Fig. 2.6 (a)	20
2.7 (a)	Input joint image with multiple target and non-target objects	21
2.7 (b)	Classical JTC output of Fig. 2.7 (a)	21
2.8 (a)	Input joint image with multiple identical targets and non-target objects	
2.8 (b)	Classical JTC output after image subtraction of Fig. 2.8 (a)	24
2.9 (a)	Input joint image with multiple identical targets and multiple non-target objects	24
2.9 (b)	FJTC output of fig. 2.8 (a) with $C=1$ and $D=1e-1$	26
2.9 (c)	FJTC output fig. 2.8 (a) with $C=1$ and $D=1e-4$	27
2.9 (d)	FJTC output fig. 2.8 (a) with $C=1$ and $D=1e-9$	28
3.1(a)	Input joint image with multiple targets and non-targets	32
3.1(b)	Unnormalized correlation output for joint image with varying illumination	33
3.2(a)	Input joint image with multiple targets with varying illumination	34
3.2(b)	Correlation output for four targets with varying illumination	34
3.3(a)	Architecture of the proposed NJTC scheme	37

3.3(b)	First and second input planes with the joint images	38
3.3(c)	Output planes with correlation distribution	40
3.4(a)	Input joint image with multiple targets and non-target	41
3.4(b)	First input plane distribution containing the reference and input joint image	42
3.4(c)	Second input plane distribution containing the square of the input image and the support of the reference	42
3.4(d)	First correlation output plane distribution	43
3.4(e)	Second correlation output plane distribution	43
3.4(f)	Normalized correlation output for joint image with varying illumination	44
3.5(a)	Input joint image with multiple targets with varying illumination	45
3.5(b)	Normalized correlation output for four targets with varying illumination	45
3.6	Negative exponential function	46
3.7(a)	Two delta like peaks represents the two targets and the non targets peaks are diminished significantly.	47
3.7 (b)	Four delta like peaks represent the four illumination varying targets.	48
3.8(a)	Gray scale image of Lena	52
3.8(b)	Input joint image with multiple targets with varying illumination and the reference.	53
3.8(c)	First correlation output plane distribution	53
3.8(d)	Second correlation output plane distribution	54
3.8 (e)	Normalized correlation output without post processing	54
3.8 (f)	Normalized correlation output with post processing	55
3.9 (a)	Image of the target car	56
3.9 (b)	Image of the non-target car	57

3.9(c)	Input joint image with multiple targets and non-target with varying illumination and the reference.	57
3.9 (d)	Normalized correlation output without post processing	58
3.9 (e)	Normalized correlation output with post processing	58
3.10 (a)	Joint image with an additive white noise of 0dB	60
3.10 (b)	Corresponding correlation output an additive white noise of 0db.	61
3.10 (c)	Normalized correlation output SNR of 5dB.	61
3.10 (d)	Normalized correlation output SNR of -5dB.	62
3.10 (e)	Post processed normalized correlation output SNR of 0dB.	62
3.10 (f)	Post processed normalized correlation output SNR of 5dB.	63
3.10 (g)	Post processed normalized correlation output SNR of -5dB.	63
3.11 (a)	Joint image with an additive white noise of 0dB	65
3.11 (b)	Correlation output an additive white noise of 0dB without post processing	65
3.11 (c)	Correlation output an additive white noise of 0dB with post processing	66
3.12 (a)	Input scene image with an additive white noise of 0dB	68
3.12 (b)	Normalized correlation output without post processing for SNR=0dB	68
3.12 (c)	Normalized correlation output with post processing for SNR=0dB	69
3.13(a)	First and second input planes with the joint images	72
3.13(b)	Output planes with correlation distribution	73
3.14(a)	Input joint image with multiple targets and non-targets	74
3.14(b)	Modified normalized correlation output of input joint image with multiple targets and non-targets before post processing.	75
3.14(c)	Modified normalized correlation output of input joint image with multiple targets and non-targets after post processing.	75

3.15(a)	Modified normalized correlation output of input joint image with multiple targets only before post processing.	76
3.15(b)	Modified normalized correlation output of input joint image with multiple targets only after post processing.	77
3.16(a)	Modified correlation output of gray level images without post processing.	78
3.17(a)	Modified correlation output of noisy input scene with only targets.	79
3.17(b)	Modified correlation output of noisy input scene with targets and non-targets present.	80
3.17(c)	Modified correlation output of noisy input scene with gray level images.	80

LIST OF ABBREVIATIONS

CCD	Charge coupled device
CPI	Correlation peak intensity
FAF	Fringe-adjusted filter
FJTC	Fringe-adjusted joint transform correlator
FWHM	Full width at half maximum
GFJTC	Generalized fringe-adjusted joint transform correlator
JPS	Joint power spectrum
JTC	Joint transform correlator
MACE	Minimum average correlation energy filter
MTDA	Multi-target detection algorithm
NJTC	Normalized joint transform correlator
PCR	Peak to clutter ratio
POF	Phase only filter
PSR	Peak to side lobe ratio
SDF	Synthetic discriminant function
SLM	Spatial light modulator
VLC	VanderLugt Correlator

LIST OF SYMBOLS

λ	Wavelength of collimated light in JTC scheme
\mathfrak{F}	Fourier transform operation
\mathfrak{F}^{-1}	Inverse Fourier transform operation
\otimes	Correlation operation
$*$	Complex conjugate operation
f	Focal length of lenses
\times	Multiplication operation
x, y, x', y'	Space domain variable
u, v	Fourier domain variable
D	FAF filter parameters

ACKNOWLEDGEMENT

The author would like to express his profound gratitude to his supervisor Dr. Satya Prasad Majumder, Professor, Department of Electrical and Electronic Engineering, Bangladesh University of Engineering and Technology (BUET), Dhaka-1000, for his guidance, suggestions, questions and supervision throughout the work. The whole-hearted co-operation of Dr. Satya Prasad Majumder made this work completed timely and successfully.

The author is also very much grateful to Dr. M. Nazrul Islam, Associate Professor, Department of Electrical and Electronic Engineering, Bangladesh University of Engineering and Technology (BUET), Dhaka-1000, for his ideas, insights and enthusiasm; those were great help in stimulating the thought and in bringing this research forward.

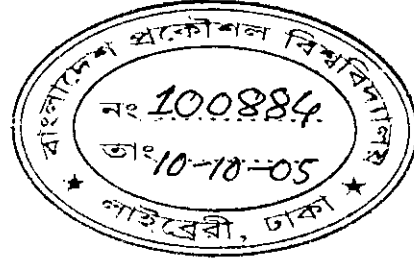
The author is grateful to Bangladesh University of Engineering and Technology, Dhaka-1000, for providing various resources required for this work. The author would also like to thank all others who extended their hands directly and indirectly to complete this work. specially Md. Rafiqul Haider, Assistant professor, Department of Electrical and Electronic Engineering, Bangladesh University of Engineering and Technology (BUET), Dhaka-1000. The author would also like to express profound gratitude to his family members and relatives for their unwavering support and encouragement during the graduate studies.

ABSTRACT

This thesis is concerned about the detection or pattern recognition of unsegmented targets under varying illumination with the application of normalized joint transform correlation technique. When the illumination within a scene cannot be controlled, the outputs for similar targets can be quite different. Pattern recognition techniques usually use the correlation operation to detect targets by means of a threshold on the correlation plane. But as correlation peak height is proportional to target intensity, high intensity non-targets can cause false alarms and dark objects can also be missed. A number of methods have been so far introduced for detection of targets under transformation of intensity. Phase only and synthetic discriminant functions have been proposed for normalization which is realized in the frequency domain. In this thesis work, an efficient implementation of normalized correlation in the space domain has been proposed to achieve real time discrimination between intensity varying similar non-targets. The previous method like complementary reference joint transform correlator was proposed which is useful in recognizing only binary images. But this scheme works almost successfully for binary and gray level images. Some researchers also pointed out that the morphological correlation is intensity invariant only when the object is brighter than the reference. But the proposed scheme has better processing speed as it utilizes linear correlation than that of morphological correlation, which is slower in computation. In this work, a high performance optical correlator has been developed which gives almost equal correlation peaks for all the targets, whether the targets are brighter or darker than the reference and whether there is noise in the input scene or not. To achieve higher discrimination ration between dissimilar non-target objects a post processing technique has also been introduced. Computer simulation shows satisfactory performance of the proposed scheme in getting intensity invariant pattern recognition.

Chapter 1

INTRODUCTION



1.1 Introduction

Pattern recognition technique is mainly concerned with the automatic detection and classification of objects. It is used for both data preprocessing and decision making. It deals with the detection and identification of a desired pattern or target in an unknown input scene, which may or may not contain the target, and with the determination of the spatial location of the targets. Pattern recognition is a rapidly developing technology with cross-disciplinary interest and participation. It overlaps with other areas such as artificial intelligence, neural modeling, adaptive signal processing and systems, estimation theory, fuzzy sets etc. Some of the major applications of pattern recognition techniques include target detection, computer vision, radar signal classification, image and speech preprocessing, face recognition, biometric identification, medical diagnosis etc.

Pattern recognition is based on patterns. A pattern can be as basic as a set of measurements or observations, perhaps represented in vector or matrix notation. Here the input is an image while the output is a decision signal based on some characteristic features of the input. Characteristic features of a pattern are any extractable measurement used. Features may result from applying a feature extraction algorithm or operator to the input data. The number of characteristic features is virtually always chosen to be fewer than the total necessary to describe the complete target and thus there is a loss of information. It is different from image processing where the input is an image and the output is also an image. Since pattern recognition is fundamentally an information reduction process, it is therefore not possible to reconstruct the original pattern but to make a precise decision [1-2].

Human being and a machine classify objects by quite different methodologies. The main difference between human and machine intelligence comes from the fact that humans perceive everything as a pattern, whereas for a machine everything is data. Without any pattern, it is very difficult for a human being to remember and reproduce the data later. Thus the storage and recall operations in human beings and machines are performed by different mechanism. [3]

1.2 Classification of Pattern Recognition Tasks

The fundamental information for pattern recognition tasks is provided through the underlying and quantifiable statistical basis for generation of patterns and the underlying structure of the pattern, provide. Based on these, there are three major groups to pattern recognition.

1.2.1 Statistical Pattern Recognition

A statistical basis for classification of algorithms is used in this approach. A set of characteristic measurements is extracted from the input data and is used to assign each feature vector to one of the classes. Features are assumed generated by a state of nature, and therefore the underlying model is a state of nature or class-conditioned set of probabilities or probability function. Various methods for finding decision functions in decision theoretic approach are matching, optimum statistical classifier and neural networks. There are two ways of matching- one is minimum distance classifier and the other is matching by correlation [4].

1.2.2 Syntactic Pattern Recognition

The significant information in a pattern may not merely be in the presence or absence of features. Rather, the interrelationships or interconnections of the features yield

important structural information, which facilitates structural description or classification. This is the basis of syntactic pattern recognition. Typically, syntactic pattern recognition approaches formulate hierarchical descriptions of complex patterns built up from simpler sub-patterns. These sub-patterns or building blocks are called primitives whereas features are any measurements.

1.2.3 Neural Pattern Recognition

The alternative of neural computing emerged from attempts draw on knowledge of how biological neural systems store and manipulate information. This leads to a class of artificial neural systems termed neural networks. For pattern association applications neural networks are particularly suited.

1.3 Implementation Techniques of Pattern Recognition

Implementation of pattern recognition techniques can be done either by a computer or by an optical system. Signal processing through computer for traditional pattern recognition has the temporal advantage, whereas optical system has an additional manipulation advantage. Most of the digital pattern recognition techniques suffer from implementation difficulties and slow processing speed. But, optical pattern recognition techniques inherently provide parallelism, ultrahigh processing speed, non-interfering communication and massive interconnection capability. Therefore, for real time pattern recognition, optical pattern recognition technique offers itself as a suitable candidate and it is a better approach than the conventional digital pattern recognition technique [5].

1.4 Optical Pattern Recognition

Optical pattern recognition uses correlation, which can be performed efficiently with the help of a lens. Correlation is a sensor independent approach that generally does not require data specific operation. The throughput of a correlator generally depends on the dimensions of the image. So complexity of the system depends on the input image size but not on the number of objects in the scene. This avoids the computational bottlenecks faced by some other techniques due to scene complexity, clutter and no of objects present. The concept of correlation pattern recognition comes from the fields of signals and systems, statistical pattern recognition and Fourier optics.

The Fourier transform properties of lens are usually used to perform optical correlation. If an input image is placed at the front focal plane of a lens and illuminated by a laser source, then the Fourier transform of the input image will be got at the back focal plane of the lens [6-7]. To perform the correlation between reference and target image, a joint image containing reference and target images placed side-by-side is placed at front focal plane of a lens. At the back focal plane, the Fourier transform of reference and target images are multiplied in the frequency domain, which is equivalent to convolution in the spatial domain. A second lens is used to transform the frequency function back to spatial domain. Other than lens, the optical devices that are used for optical pattern recognition technique are Spatial light modulator (SLM), charge coupled device (CCD), mirror, beam splitter, laser etc. Since an optical correlator provides parallel processing capability, it is a suitable candidate to provide better speed advantages compared to digital counter parts and can be used for real time target detection process.

There are two widely used optical correlators namely VanderLugt Correlator (VLC) and Joint Transform correlator (JTC).

1.4.1 VanderLugt Correlator (VLC)

VanderLugt Correlator was first introduced in 1964 and it is also known as matched filter based correlator [8-13]. This filter must be accurately aligned along the optical

axis and slight mismatch results in output intensity degradation for optical correlation operation [14-16]. Hence it is not suitable for real time operation. If an input signal is placed at the input plane and illuminated by a point laser source, the complex light field distribution produced at the output plane is given by Fourier transform operation. The phase fronts of the wave coming from input plane and incident on output are both curved and distorted. The phase transmittance of the matched filter the plane output plane must be the conjugate match to the phase of the Fourier transform of the input. As a result, the phase variations of the beam incident on output plane is cancelled and the resulting distribution becomes a parallel beam. Lens performs the inverse Fourier transform and produces the output plane. If the input is different the phase-front will not exactly be cancelled by the filter and the light distribution in output will produce a spot of poor intensity or no spot at all. The complex light distribution at third plane can be expressed as inverse Fourier transformation. If the input object is moved laterally in the input plane, the Fourier transform remains fixed in space but multiplied by a phase factor that depends on the lateral movement. The intensity of bright correlation spot is proportional to the degree to which the input and the filter functions are matched. This correlation system provides a great deal of sensitivity since it is both phase matched and amplitude matched. Since the system is linear and superposition theorem holds, it is also valid for multiple objects present at different at different locations of the input plane.

1.4.2 Joint Transform Correlator (JTC)

Joint transform correlator is a device consisting of two optical systems in which two signals are simultaneously transformed to produce their spectra, and these spectra are multiplied and inverse Fourier transformed to produce the correlation output.

Joint transform correlation (JTC) was first introduced by Goodman, in 1966 [17]. With the development of electronically addressable spatial light modulator (SLM), JTC has been introduced as a real-time programmable optical pattern recognition technique [18].

JTC does not require any complex matched filter fabrication and accurate alignment of the filter along the optical axis. It uses a spatial (impulse response) domain filter. Although a classical JTC provides many attractive advantages, it is found to suffer from large correlation side-lobes, large correlation width, wide zero order peak and low optical efficiency [18-19]. In contrast to VLC, joint transform power spectrum in JTC is dependent on input signal. Some of the major advantages of JTC are that it allows real-time update of the reference image and permits parallel Fourier transform of the reference image and the unknown input scene.

Binary JTC has been proposed to improve the performance of classical JTC. A binary JTC is found to be superior to a classical JTC in terms of the correlation peak intensity, correlation width and discrimination sensitivity [20-22]. However, a binary JTC involves computationally intensive Fourier plane joint power spectrum (JPS) binarization, which limits the system processing speed [23]. Again the binary JTC cannot completely eliminate the strong zero-order term at the output plane. For multi-object input scene, in particular, the JPS binarization process introduces harmonic correlation peaks that may cause spurious correlation peaks and thus, results misses [24-25] and thereby complicating the target detection process.

Different zero-order elimination techniques have been proposed in the literature to improve the performance of the JTC [27-32]. DC blocking, using an opaque aperture to block the dc component can be easily carried out. But, when the input scenes are noised, zero order items become very complicated which results in the futility of the method. Fourier plane image subtraction [28], correlation plane image subtraction [29] and phase-shift power spectrum subtraction [30] all can yield a better correlation output. All of the methods need multiple processing steps to achieve it, which limits their applications to the highly required real-time recognition tasks.

The above-mentioned JTCs still produce relatively broad correlation peaks which complicates their application to multiple target detection process. To get a sharper

correlation peaks, one of the recent approaches is the use of a fringe adjusted JTC (FJTC) based on Newton-Raphson algorithm [33]. Fringe adjusted filter (FAF)-based JTC avoids many problems otherwise associated with other JTC techniques. In FJTC technique, the JPS is multiplied by the transfer function of FAF before inverse Fourier transformation. This technique yields better correlation performance than alternate JTCs for the noise free single and multi-target binary input scenes under normal as well as poor illumination conditions [34]. However, for noise corrupted input scenes, whenever the reference power spectrum contains very low values, the FJTC technique may suffer from low correlation output. To overcome this problem, a fractional power fringe adjusted JTC has been proposed for single target detection. This technique employs a family of real valued filters, called generalized fringe adjusted filters (GFAF) [35]. By adjusting a parameter, one can obtain classical JTC, fringe adjusted JTC and phase-only JTC without actually fabricating these complex valued filters. It is found that the phase only JTC provide better noise robustness than all of them.

Various other non-linear joint transform correlator have been also proposed for optical pattern recognition among which all-optical photo refractive crystal based JTC have been found to be particularly attractive [37-40]. However all of the above methods utilize at most half of the input and output plane SLM and therefore provides poor utilization of space bandwidth product. Again, multi-step processing techniques to eliminate the extraneous signals, limit their operation in such cases where processing speed is a crucial constant. To overcome the above-mentioned problem, a phase encoding principle has been adopted with FAF [36] to get a sharper and only a single correlation peak per target. This phase encoding operation is performed in such a way that it does not have any detrimental effect on the system processing speed. This technique uses separate reference and input planes and yields one correlation peak per target instead of a pair of peaks thus ensuring better utilization of space bandwidth product [41-43].

1.5 Intensity Invariant Pattern Recognition

When the illumination within a scene cannot be controlled, the outputs for similar targets can be quite different. Correlation peak height is proportional to the target intensity. Because detection is often determined by means of a threshold on the correlation plane, dark objects can be missed. However, high intensity image clutter can cause false alarms. Very few methods have been so far introduced for detection of targets under transformation of intensity [44-45]. Phase only and synthetic discriminant functions have been proposed for normalization which is realized in the frequency domain [46]. Complementary reference joint transform correlator is useful in recognizing only binary images [47]. Intensity invariant recognition using the sliced orthogonal nonlinear generalized correlation has been also introduced [48]. Recently, some researchers pointed out that, the morphological correlation is intensity invariant when the object is brighter than the reference [49-50]. Here normalized correlation in the space domain has been developed to achieve real time discrimination under varying illumination.

1.6 Objectives of the Thesis

The objective of this work is to develop a method for getting intensity invariance optical pattern recognition in real time and to apply the Cauchy-Schwarz inequality to correlation filters that will result in normalization to achieve intensity invariance. Further, to develop a modified recognition algorithm that will produce prominent detection signal between intensity varying similar non-targets and noise. Finally a post processing technique will be introduced for better discrimination. In this thesis, a efficient optical correlator will be proposed that will give almost equal correlation peaks for all the targets, whether the targets are of varying illumination and whether there is noise in the input scene or not.

1.7 Thesis Outline

This thesis consists of four chapters. In the first chapter some introduction on optical pattern recognition has been given, especially on joint transform correlation. Also a brief description of the theories and problems associated with this work has been given. Chapter 2 deals with joint transform correlation in details. Classical JTC, fringe-adjusted JTC, fractional power fringe-adjusted JTC with theory and simulation. Chapter 3 deals with the theory and simulation of normalized joint transform correlation algorithm that is a basis intensity invariant target detection. Chapter 4 is the final chapter giving a conclusive remark on this work along with some suggestive future works in this area.

Chapter 2

JOINT TRANSFORM CORRELATION TECHNIQUE

2.1 Introduction

One of the most widely used correlation technique for optical pattern recognition is the joint transform correlator (JTC) technique. In a JTC technique, the unknown input image and the reference image are placed side-by-side by using a spatial light modulator (SLM) and are illuminated by a coherent light source. Fourier transformation of the input joint image is done with the help of a lens. The Fourier transform patterns constructively interfere with each other to create an interference pattern called joint power spectrum (JPS). This joint power spectrum is recorded by a CCD camera and is further inverse Fourier transformed by using another lens to get the correlation output. If there is a match between the reference and input scene, a pair of correlation peaks or bright spots is produced. For a mismatch, negligible or no correlation peaks are produced. Several modifications to the classical JTC have been proposed to overcome the limitations it suffers from. In this chapter the classical JTC, image subtraction technique and fringe-adjusted JTC are discussed.

2.2 Classical Joint Transform Correlation Technique

The architecture of a classical JTC can be shown in Fig. 2.1. The reference image and the input images are displayed side-by-side using an SLM and are illuminated by a coherent light source. The combined light distribution passes through the first Fourier lens L_1 and the complex light distribution called JPS is recorded by a CCD array. The JPS is then introduced into the second lens and correlation output is obtained at the back focal length of the second lens. In case of fringe-adjusted JTC (FJTC), the JPS is multiplied by the real valued FAF before applying the inverse Fourier transformation to get sharp delta-like correlation peaks. In this section the theory and simulation of

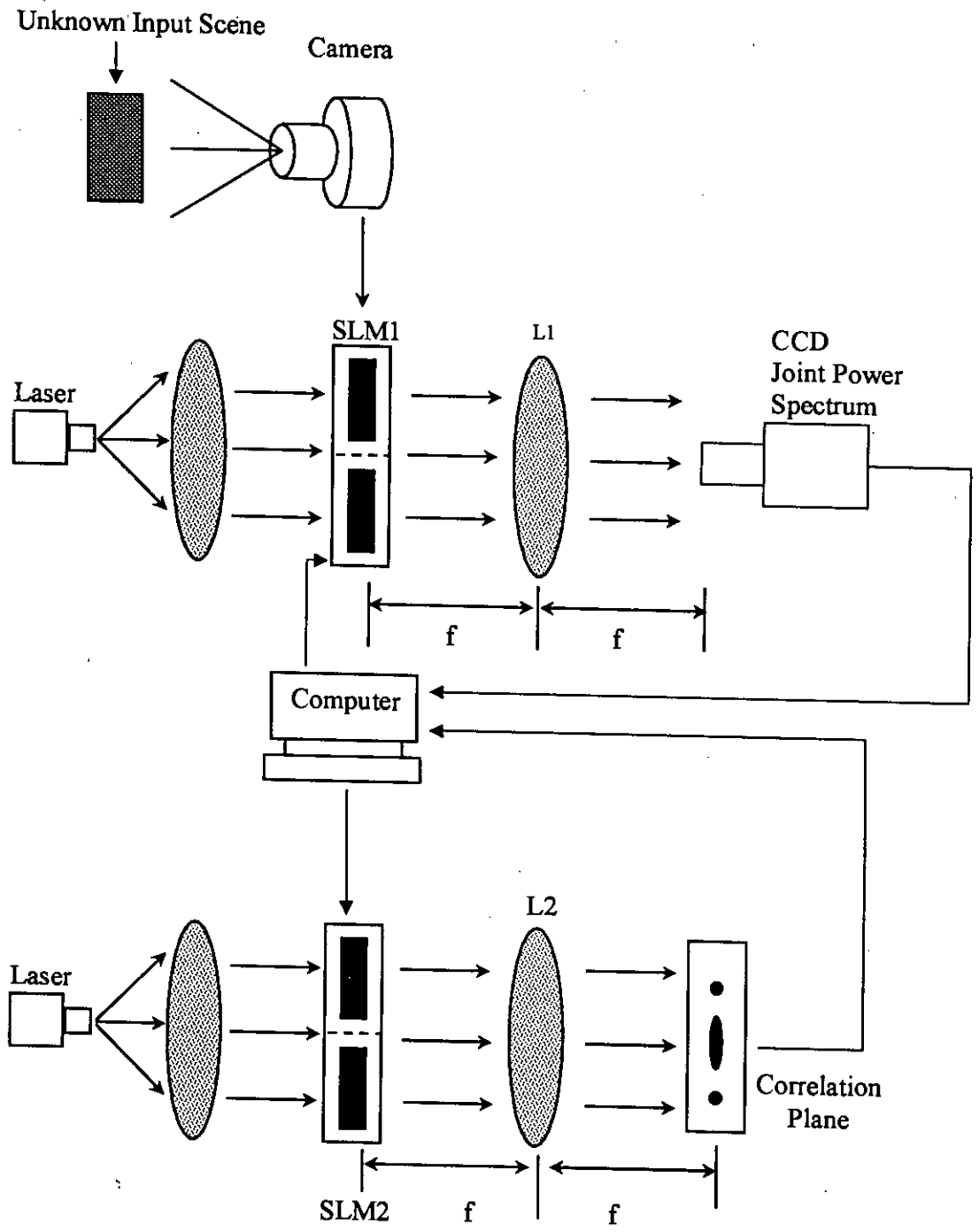


Fig 2.1 Classical JTC architecture with Image subtraction

classical JTC will be discussed first for single target detection and then for multiple target detection. Then we will discuss the FJTC and Fourier plane image subtraction technique.

2.2.1 Single Target Detection

2.2.1.1 Analysis

Let a reference image $r(x, y)$ and a target image $t(x, y)$ are displayed side-by-side in the input plane by using an SLM. With $r(x + x_0, y)$ representing the reference image and $t(x - x_0, y)$ representing the input scene in the input plane separated by a distance $2x_0$ along the x axis, the input joint image $f(x, y)$ can be expressed as

$$f(x, y) = r(x + x_0, y) + t(x - x_0, y) \quad (2.1)$$

Lens L1 performs the Fourier transform of $f(x, y)$ to yield

$$F(u, v) = |R(u, v)| \exp[j\Phi_r(u, v) + jux_0] + |T(u, v)| \exp[j\Phi_t(u, v) - jux_0] \quad (2.2)$$

where $R(u, v)$ and $T(u, v)$ are the amplitudes, $\Phi_r(u, v)$ and $\Phi_t(u, v)$ are the phases of the Fourier transforms of $r(x, y)$ and $t(x, y)$, respectively; u and v are mutually independent frequency domain variables scaled by a factor of $\frac{2\pi}{\lambda}$, λ is the wavelength of collimating light, f is the focal length of lenses L1 and L2. The complex light distribution produced in the back focal plane of L1, called the JPS, is then detected by a square-law device such as a CCD array. The JPS is given by

$$\begin{aligned} |F(u, v)|^2 &= F(u, v) \cdot F^*(u, v) \\ &= |R(u, v)|^2 + |T(u, v)|^2 + 2|R(u, v)||T(u, v)| \times \cos[\Phi_r(u, v) - \Phi_t(u, v) + 2ux_0] \end{aligned} \quad (2.3)$$

In a classical JTC, this JPS is introduced into second SLM which is illuminated by another laser of same frequency. Lens L2 performs the inverse Fourier transformation of the JPS to yield the correlation output. The final output can be expressed as

$$o(x', y') = r(x', y') \otimes r^*(x', y') + i(x', y') \otimes i^*(x', y') \\ + r(-x' - 2x_0, -y') \otimes i^*(-x', -y') + r^*(x' - 2x_0, y') \otimes i(x', y') \quad (2.4)$$

From Eq. (2.4), it is evident that the correlation output contains autocorrelation of the reference image and the input scene objects and cross-correlation between the reference image and the input scene objects. The first and second terms of Eq. (2.4) produce the zero-order peak and the third and fourth term generates the desired cross correlation peaks around $(0, -2x_0)$ and $(0, 2x_0)$ respectively.

2.2.1.2 Simulation Results

To analyze the performance of a classical JTC, a binary character 'H' of English Alphabet has been taken as the reference image. The size of the character is 32×32 pixels and it is placed in a joint image of size 256×256 pixels. The joint image also contains a target image. The simulations are performed using FFT2 routine of MATLAB software and the outputs are plotted using the 3-D plotting routine.

In Fig. 2.2 (a), the target image is the same as the reference image 'H' and the corresponding classical JTC output is shown in Fig 2.2 (b). From the figure, it is evident that there is the presence of a strong zero-order term at the middle of the output plane and a pair of correlation peaks is produced for the target object.

The same analysis has been made with a non-target image 'T' for the same reference image 'H' as shown in Fig. 2.3. In this case a pair of correlation peaks is obtained with negligible intensity.

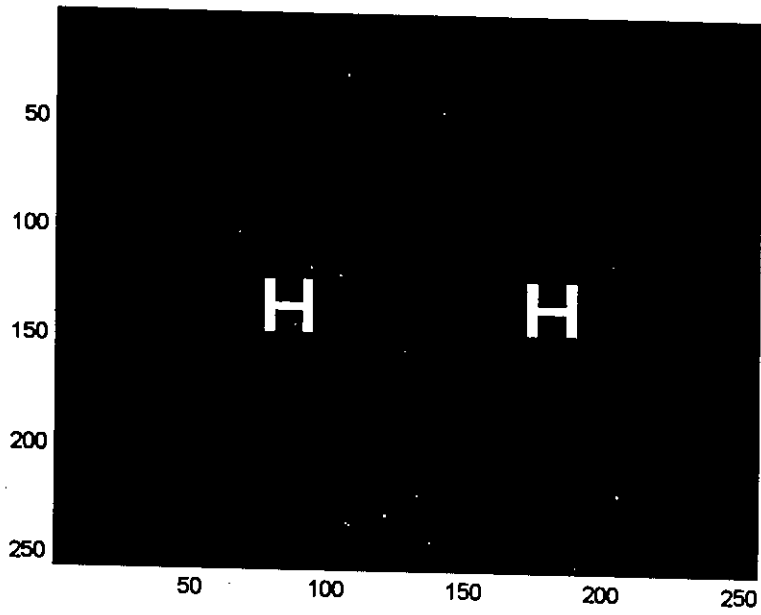


Fig. 2.2 (a) Input joint image of identical target object

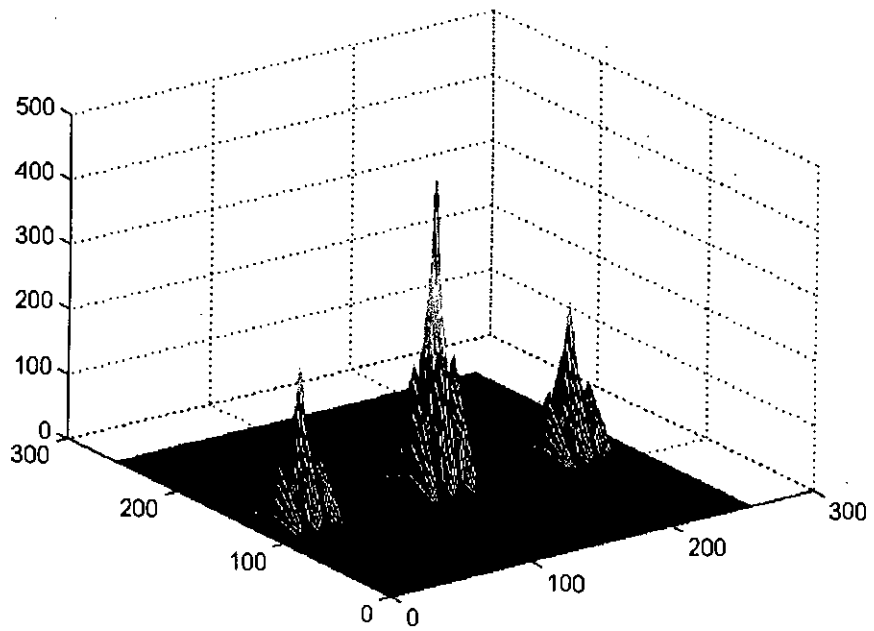


Fig. 2.2 (b) Classical JTC output of Fig. 2.2 (a)



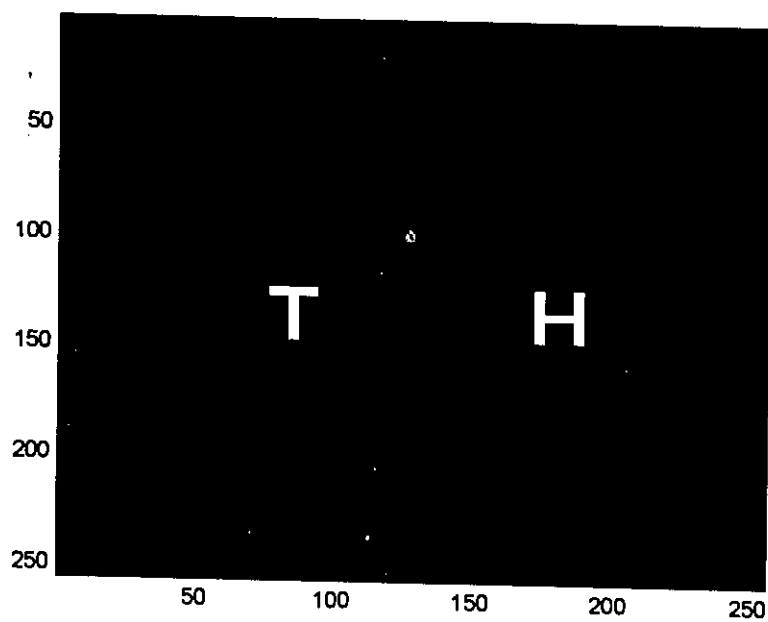


Fig. 2.3 (a) Input joint image of non-target object

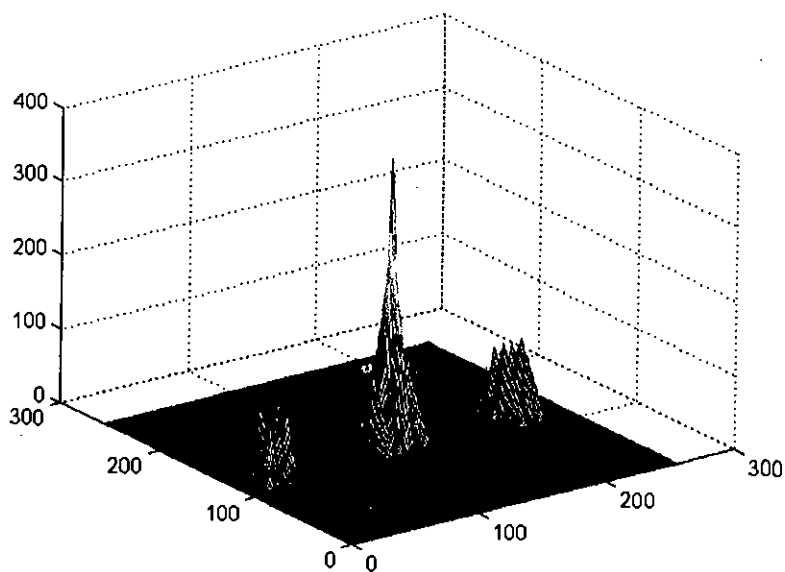


Fig. 2.3 (b) Classical JTC output of Fig. 2.3 (a)

From the Fig 2.2(b) it is observed that there is a DC term or strong zero order term at the center of the output plane and a pair of cross-correlation peak indicating the presence of the target. The DC term that is obtained at the center of the output plane with a very high correlation peak intensity compared to the target peaks which deteriorates the detection process and lowers the optical efficiency. The position of the zero-order term is always fixed i.e. at the center of the correlation plane. The positions of the two cross-correlation peaks are such that one is at the exact location of the target and the other one is at the mirror position of the target. Locations of the correlation peaks depend on the relative placement of the input and reference image in the joint image. The height of the cross-correlation peaks indicates the degree of similarity between the reference image and the target images present in the input scene. The same analysis has been made with the non target image 'T' with the same reference 'H' as shown in Fig 2.3. In this case a pair of correlation peaks is obtained for the non-target, but with negligible peak intensity.

2.2.2 Multiple Target Detection

2.2.2.1 Analysis

If $r(x, y + y_0)$ represents the reference image and $t(x, y - y_0)$ represents the input scene containing n objects $t_1(x - x_1, y - y_1)$, $t_2(x - x_2, y - y_2)$, $t_n(x - x_n, y - y_n)$, the input joint image may be expressed as

$$f(x, y) = r(x, y + y_0) + \sum_{i=1}^n t_i(x - x_i, y - y_i) \quad (2.5)$$

Applying Fourier transform to the input joint image by the lens L1 yields

$$F(u, v) = |R(u, v)| \exp[j\Phi_r(u, v) + jvy_0] + \sum_{i=1}^n |T_i(u, v)| \exp[j\Phi_n(u, v) - jux_i - jvy_i] \quad (2.6)$$

where $R(u, v)$ and $T(u, v)$ are the amplitudes, $\Phi_r(u, v)$ and $\Phi_n(u, v)$ are the phases of the Fourier transforms of $r(x, y)$ and $t_i(x, y)$, respectively; u and v are mutually independent frequency domain variables scaled by a factor of $\frac{2\pi}{\lambda}$, λ is the wavelength of collimating light, f is the focal length of lenses L1 and L2. The complex light distribution produced in the back focal plane of L1, called the JPS, is then detected by a square-law detector such as a CCD array. The JPS is given by

$$|F(u, v)|^2 = |R(u, v)|^2 + \sum_{i=1}^n |T_i(u, v)|^2 + 2 \sum_{i=1}^n |T_i(u, v)| |R(u, v)| \cos[\Phi_n(u, v) - \Phi_r(u, v) - ux_i - vy_i - 2vy_0] + 2 \sum_{i=1}^n \sum_{k=1, k \neq i}^n |T_i(u, v)| |T_k(u, v)| \cos[\Phi_n(u, v) - \Phi_{ik}(u, v) - ux_i + ux_k - vy_i + vy_k] \quad (2.7)$$

From Eq. (2.7), it is evident that the correlation output contains autocorrelation of the reference image and the input scene objects, cross-correlation between the reference image and the input scene objects, and cross-correlations between different input scene objects. The first term produces the auto-correlation of the reference image only while the second term produces the same for different input scene image only. The fourth term produces the cross-correlation between different input scene images without considering the reference image. Therefore, the first and second term of Eq. (2.7) produce the strong zero-order peak and the fourth term produces the false correlation peaks, which are called false alarms. Only the third term generates the desired correlation peaks between the reference image and different input scene images.

2.2.2.2 Simulation Results

To simulate the performance of a classical joint transform correlator in case of multiple objects (target and non-targets) present simultaneously in the input scene, the same 256×256 zero-padded image matrix is taken for the input scene. 'H' is considered reference in each case.

Two target images 'H' are placed at the left side of the joint image as shown in Fig 2.4 (a). The classical JTC output of Fig 2.4 (a) is shown in Fig 2.4 (b). The correlation output shows the strong zero-order peak at the center. Two pairs of cross-correlation peaks indicate two target images. But another pair of auto-correlation peaks between the targets produces the false alarm.

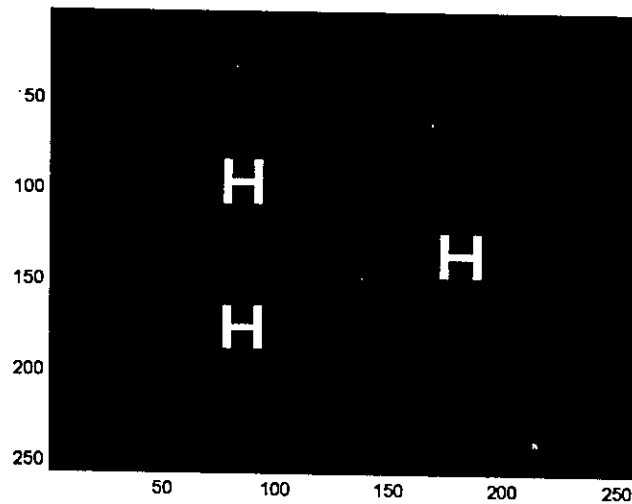


Fig 2.4 (a): Input joint image with identical targets

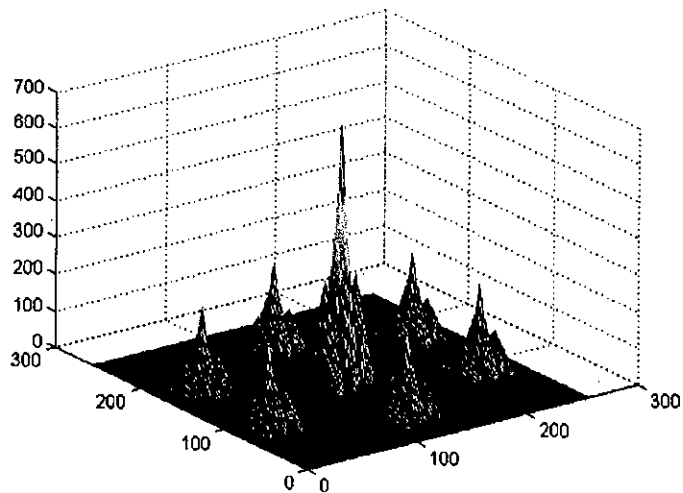


Fig. 2.4 (b): Classical JTC output of Fig. 2.4 (a)

Two non-target image 'T' and 'A' are the input scene objects placed at the left side of the joint image as shown in Fig 2.5(a). The joint image is processed and the correlation output is given in Fig 2.5(b). The correlation output shows a strong zero order term, two pairs of cross correlation peaks for the non targets and reference and a pair of cross correlation peaks between the non-targets. These cross correlation peaks are of small amplitude.

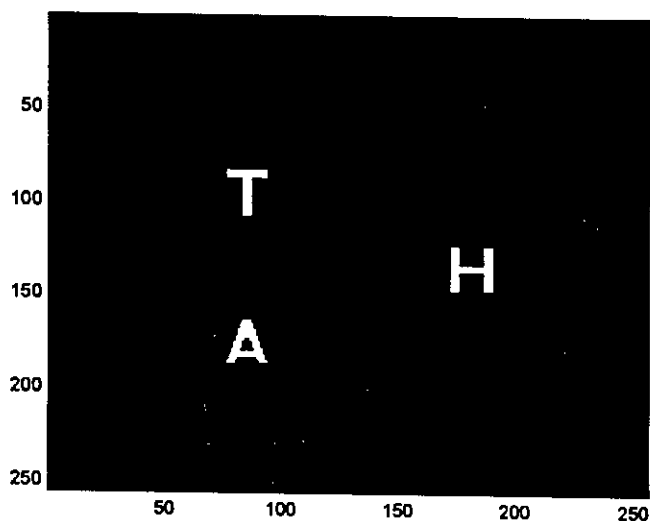


Fig 2.5 (a): Input joint image with two non targets

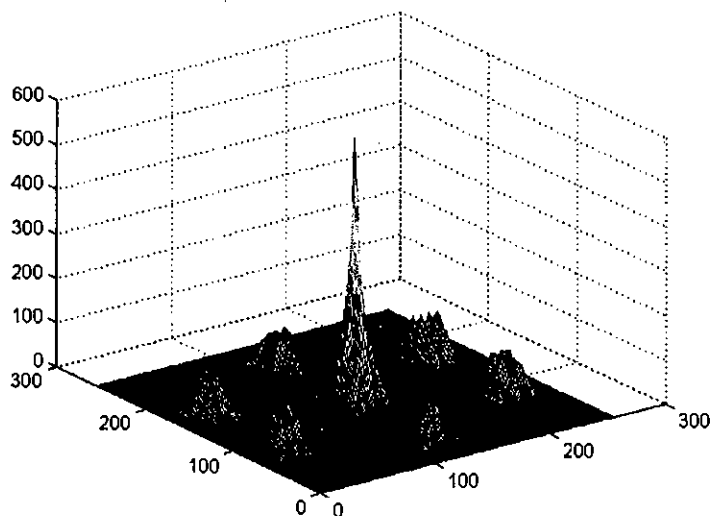


Fig. 2.5 (b): Classical JTC output of Fig. 2.5 (a)

One target image 'H' and one non-target image 'A' are the input objects placed at the left side of the joint image as shown in Fig 2.6 (a). The joint image is processed to find the correlation output of Fig 2.6 (b). The correlation output shows a strong zero-order peak, a pair of cross-correlation peaks for the target, a pair of cross-correlation peak for the non-target (which is smaller than the target peak) and a pair of cross-correlation peaks between the target and non-target.

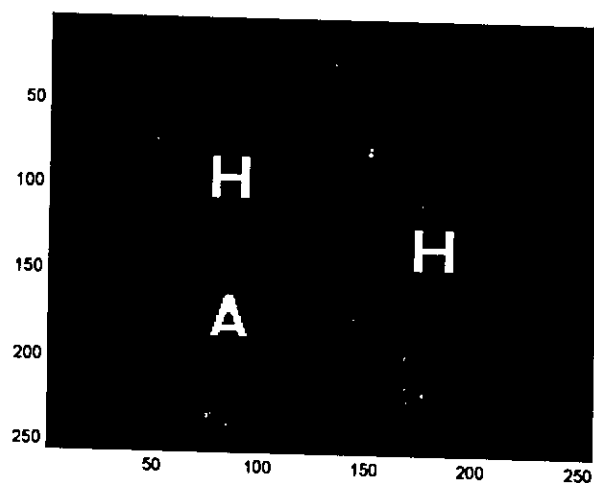


Fig 2.6 (a): Input joint image with one target and one non-target

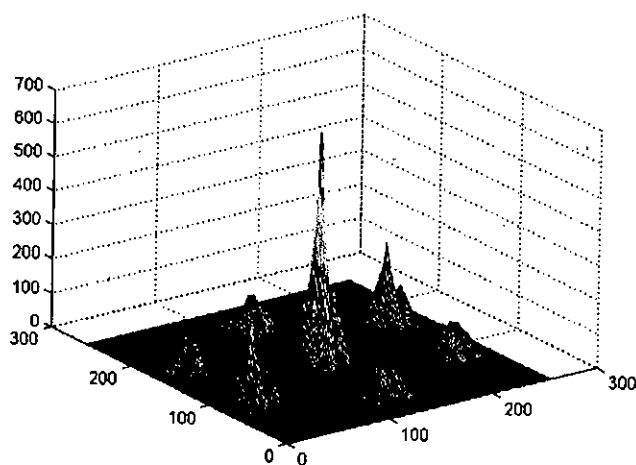


Fig. 2.6 (b): Classical JTC output of Fig. 2.6 (a)

Multiple target images and multiple non-target images are the input objects placed at the left side of the input plane as shown in Fig 2.7 (a). The joint image of Fig 2.7 (a) has been processed to find the correlation output of Fig 2.7 (b). The correlation output shows the strong zero-order peak at the center of the output plane. It also shows several cross-correlation peaks for the targets and non-targets and several auto-correlation peaks among the target and non-target objects. Due to the presence of strong false alarms, it is quite difficult to locate the actual position of the target images.

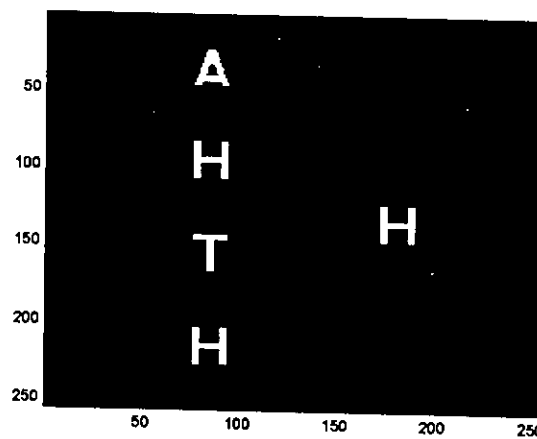


Fig 2.7 (a): Input joint image with multiple target and non-target objects

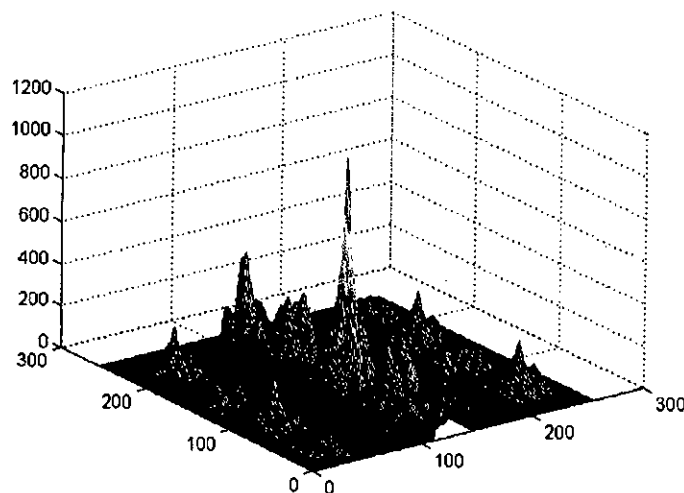


Fig. 2.7 (b): Classical JTC output of Fig. 2.7 (a)

2.3 Classical Joint Transform Correlation with Image Subtraction

2.3.1 Analysis

We can avoid the on-axis correlation distribution if the zero-order term of the joint power spectrum is eliminated. Since the zero-order correlation are derived from the individual power spectrum of $r(x, y)$ and $t(x, y)$, these power spectrum can be eliminated from the joint power spectrum by the use of computer. After subtracting these two terms from Eq. (2.3), the JPS for single object input scene becomes

$$P(u, v) = |F(u, v)|^2 - |R(u, v)|^2 - |T(u, v)|^2 \quad (2.8)$$

Now inverse Fourier transform of Eq. (2.8) produces the final correlation output as

$$g(x', y') = r(-x' - 2x_0, -y') \otimes t^*(-x', -y') + r^*(x' - 2x_0, y') \otimes t(x', y') \quad (2.9)$$

In Eq. (2.9) there are only the cross correlation terms between the reference and the target image of the input scene.

In the case of multi-object input scene, the zero-order power spectra are derived from the Fourier transformation of the reference image $r(x, y + y_0)$ and the input scene image containing targets of $t_1(x - x_1, y - y_1), t_2(x - x_2, y - y_2), \dots \dots \dots t_n(x - x_n, y - y_n)$ respectively. By subtracting the reference only power spectra and the input scene only power spectra, we get the modified JPS for multi-object input scene as given by

$$\begin{aligned} P(u, v) &= |F(u, v)|^2 - |R(u, v)|^2 - \sum_{i=1}^n |T_i(u, v)|^2 \\ &= \sum_{i=1}^n |R(u, v)| |T_i(u, v)| \exp[j(\Phi_r(u, v) - \Phi_n(u, v) + ux_i + v(y_0 + y_i))] \\ &\quad + \sum_{i=1}^n |R(u, v)| |T_i(u, v)| \exp[-j(\Phi_r(u, v) - \Phi_n(u, v) + ux_i + v(y_0 + y_i))] \end{aligned} \quad (2.10)$$

Inverse Fourier transform of Eq. (2.10) gives the correlation output for the multi-object input scene as expressed by

$$\begin{aligned}
g(x', y') = & \sum_{i=1}^n r(-x' - x_i, -y' - y_i - 2y_0) \otimes t^*(-x', -y') \\
& + \sum_{i=1}^n r^*(x' - x_i, y' - y_i + 2y_0) \otimes t(x', y')
\end{aligned} \tag{2.11}$$

In Eq. (2.11), again there are only cross-correlation terms between the reference and target images only.

The above process of subtracting the reference only power spectra and the input scene only power spectra from the joint power spectra at the Fourier plane is known as Fourier plane image subtraction technique. The Fourier plane image subtraction technique eliminates the zero-order term and other false alarms generated by the cross-correlation among different objects in the input scene.

2.3.2 Simulation Results

Fourier plane image subtraction technique is employed and simulation result is shown for the joint image as shown in Fig. 2.8 (a). The character 'H' on the right side represents the reference image and all the characters on the left side represent the input scene images. Thus the input scene contains both target and non-target objects. Fig. 2.8 (b) shows the classical JTC output of Fig. 2.8 (a) with Fourier plane image subtraction. From the figure, it is evident that the zero-order diffraction term and other false alarms are completely eliminated from the output plane and there exists only a pair of cross-correlation peaks for each input scene object. Again non-target correlation peak intensity is comparatively lower than the target object peak.

Fourier plane image subtraction technique provides better detection of target objects while eliminating the false alarms and other extraneous signals. We can also locate the reference object and input scene as closely as we wish. But still large correlation width and large correlation side lobes lowers optical efficiency of the detection scheme.

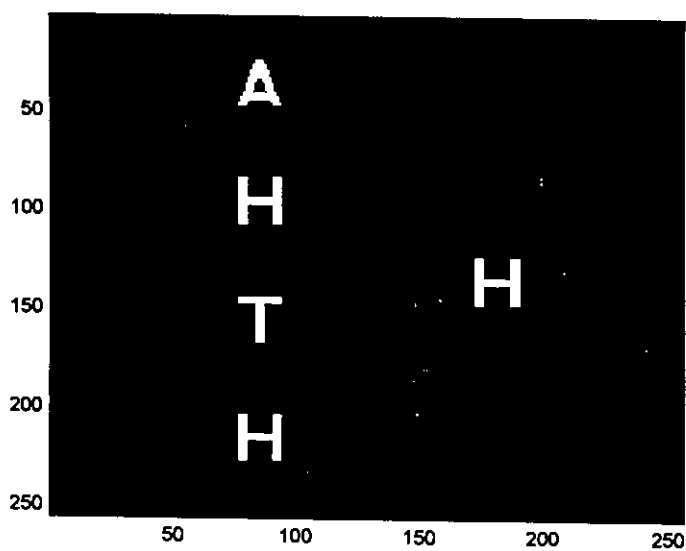


Fig. 2.8 (a): Input joint image with multiple identical targets and non-target objects

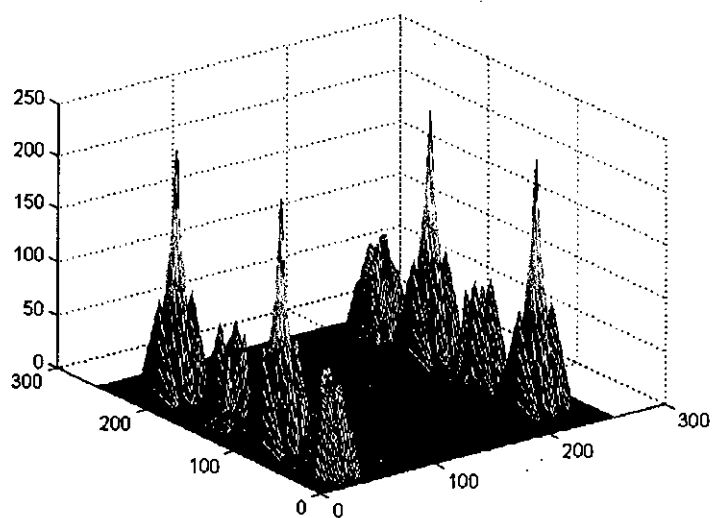


Fig. 2.8 (b): Classical JTC output after image subtraction of Fig. 2.8 (a)

2.4 Fringe-adjusted Joint Transform Correlation with Image Subtraction

2.4.1 Analysis

The classical JTC output with Fourier plane image subtraction suffers from lower optical efficiency and wide correlation peaks. To yield better correlation performance, the fringe-adjusted JTC (FJTC) technique has been proposed. In FJTC technique, the JPS is multiplied by the real valued fringe-adjusted filter (FAF) transfer function before applying the inverse Fourier transformation to get the correlation output. The transfer function of the FAF is given by

$$H_{faf}(u, v) = \frac{C(u, v)}{D(u, v) + |R(u, v)|^2} \quad (2.12)$$

where $C(u, v)$ and $D(u, v)$ are either constants or functions of u and v . When $C(u, v)$ is properly selected, one can avoid an optical gain greater than unity. With very small values of $D(u, v)$, the pole problem otherwise associated with a inverse filter is eliminated, and it is still possible to obtain a large auto-correlation peak. When $D(u, v) \ll |R(u, v)|^2$, $C(u, v)=1$, the transfer function of the FAF may be approximated as $H_{faf}(u, v) \approx |R(u, v)|^{-2}$. The function $C(u, v)$ can also be used to suppress noise or band limit the signal or both. Thus, in FJTC, the amplitude matching can be implemented more effectively to yield sharper and larger correlation peak intensity. There is no detrimental effect on system processing speed if the FAF is implemented. Because the computation associated with the FAF can be performed before the practical implementation.

For single target input scene, the modified JPS after image subtraction is multiplied by the transfer function of the FAF, $H_{faf}(u, v)$ and is thus given by

$$G_f(u, v) = H_{faf}(u, v) \times P_r(u, v) \approx |R(u, v)|^{-2} \times P_r(u, v) \quad (2.13)$$

For multiple target input scene, the modified JPS after image subtraction is multiplied by the transfer function of the FAF, $H_{\text{faf}}(u, v)$ and is thus given by

$$G_m(u, v) = H_{\text{faf}}(u, v) \times P_m(u, v) \approx |R(u, v)|^{-2} \times P_m(u, v) \quad (2.14)$$

Inverse Fourier transformation of Eq. (2.13) and Eq. (2.14) produce a pair of sharp delta-like correlation peak for each target object and almost negligible correlation peak for non-target object. Simulation results prove the effectiveness of this method.

2.4.2 Simulation Results

In order to avoid the zero-order terms and unwanted false alarms Simulation for the for the fringe-adjusted joint transform correlation has been performed with Fourier plane image subtraction. The input joint image used for the simulation purpose is shown in Fig. 2.9 (a). The simulation is done for various values of parameter $D(u, v)$ of the fringe-adjusted filter. The corresponding correlation output is shown in Fig. 2.9 (b) to Fig. 2.9(d).

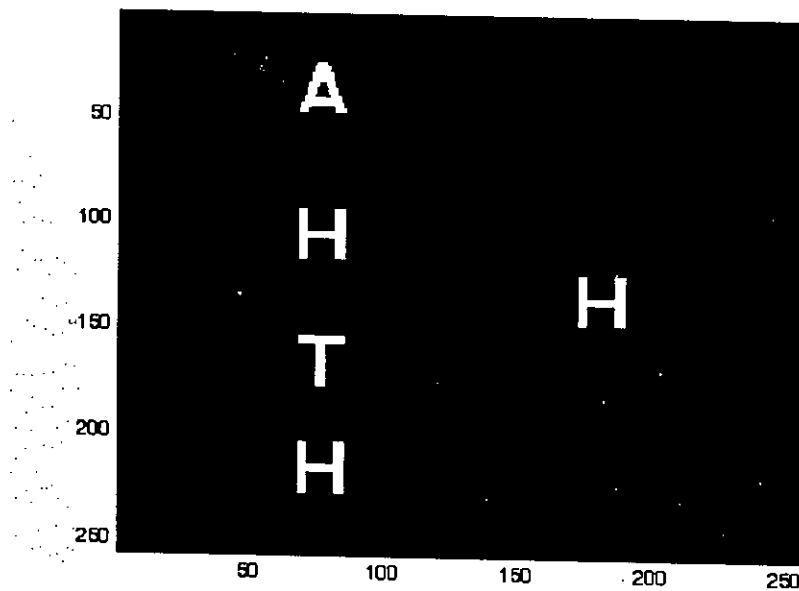


Fig. 2.9 (a): Input joint image with multiple identical targets and multiple non-target objects

We can see that from the figures the FJTC technique produces a pair of sharp delta-like correlation peak for each target and almost negligible correlation peaks for non-target objects. Again higher the value of $D(u,v)$ parameter from an optimal value, the target peaks become more and more sharper. But at the same time, the correlation plane generates spurious peaks and deteriorates the correlation performance. Therefore, selection of an optimal value of $D(u,v)$ parameter should be done by trial and error method for the best value of FAF parameters.

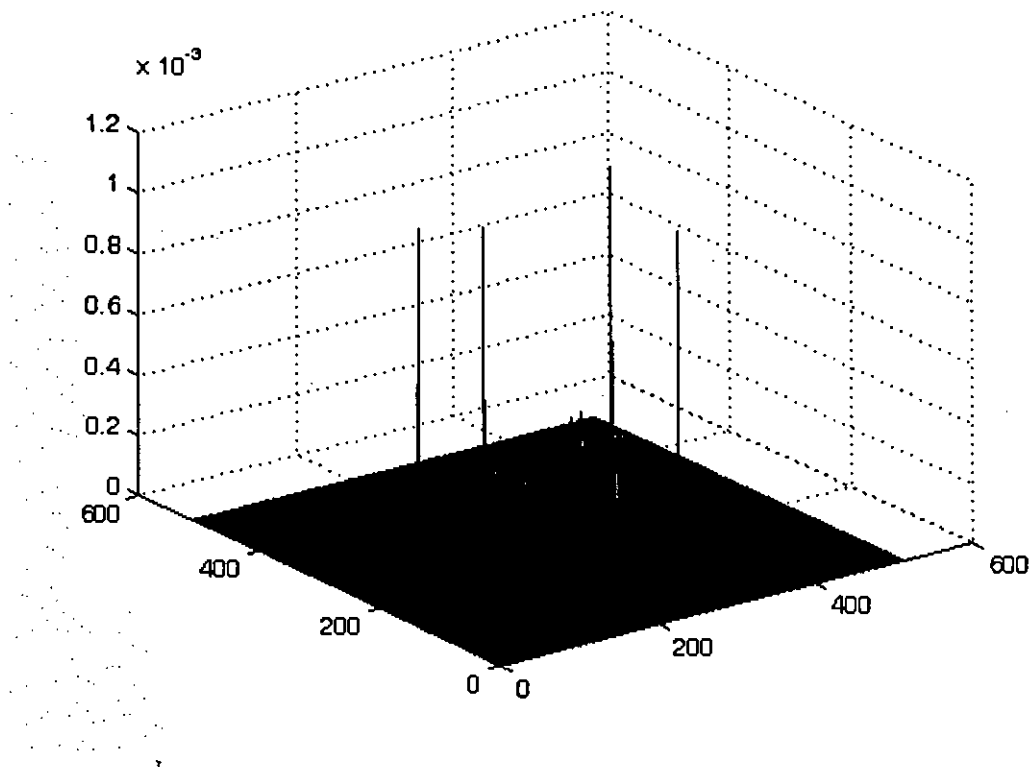


Fig. 2.9 (b): FJTC output of fig. 2.9 (a) with $C=1$ and $D=1e-1$

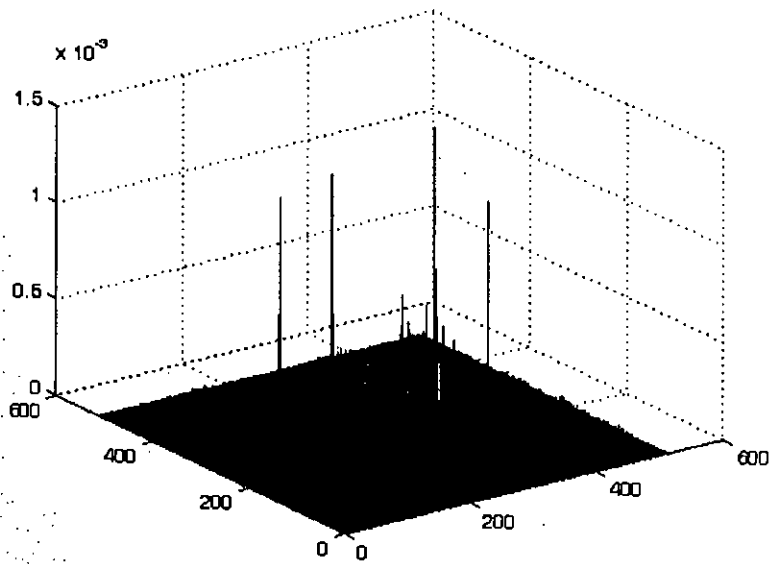


Fig. 2.9 (c): FJTC output of fig. 2.9 (a) with $C=1$ and $D=1e-4$

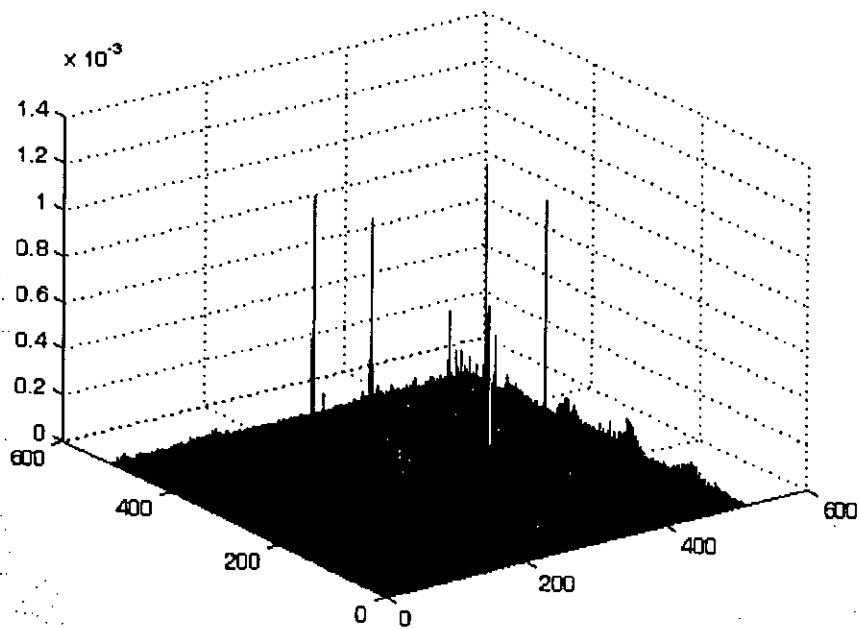


Fig. 2.9 (d): FJTC output of fig. 2.9 (a) with $C=1$ and $D=1e-9$

2.5 Conclusion

Joint transform correlation technique is used extensively for optical correlation purposes. Classical JTC is simple but it gives large correlation width, strong zero order terms and false alarm in the case of multiple object input scene. Image subtraction technique with classical JTC technique, eliminates the false alarms and zero-order terms present in the classical JTC technique. But here still the correlation peaks are wide and there is presence of side-lobes in the output plane. To overcome this problem, the modified JPS after image subtraction, is multiplied by the transfer function of a real valued fringe-adjusted filter. Incorporation of FAF, produces sharp delta-like correlation peaks for each target object and there is almost none or negligible correlation peaks for non-target objects. According to the condition of the input scene or reference image, the required JTC can be chosen. In this thesis, the concepts of the above techniques have been used.

Chapter 3

NORMALIZED JOINT TRANSFORM CORRELATION ALGORITHM

3.1 Introduction

Correlation provides a measure of similarity between a reference template and regions of the input image. This measure is dependent on the intensity variations in the input image. A high intensity image region which is quite different from the reference template can have a greater correlation value than a low intensity image region which is identical to the reference template. This will lead to false target detection. Hence intensity invariant pattern recognition is necessary.

3.2 Unnormalized Intensity Varying Multi-target Detection

3.2.1 Theoretical Analysis

If $r(x, y + y_0)$ represents the reference image and $t(x, y - y_0)$ represents the input scene containing n objects of varying illumination $t_1(x - x_1, y - y_1)$, $t_2(x - x_2, y - y_2)$, $t_n(x - x_n, y - y_n)$, the input joint image may be expressed as

$$f(x, y) = r(x, y + y_0) + \sum_{i=1}^n t_i(x - x_i, y - y_i) \quad (3.1)$$

Applying Fourier transform to the input joint image by lens yields

$$F(u, v) = |R(u, v)| \exp[j\Phi_r(u, v) + jvy_0] + \sum_{i=1}^n |T_i(u, v)| \exp[j\Phi_{t_i}(u, v) - jux_i - jvy_i] \quad (3.2)$$

where $R(u, v)$ and $T(u, v)$ are the amplitudes, $\Phi_r(u, v)$ and $\Phi_n(u, v)$ are the phases of the Fourier transforms of $r(x, y)$ and $t_i(x, y)$. The complex light distribution produced in the back focal plane of lens, called the JPS, is then detected by a square-law detector such as a CCD array. The JPS is given by

$$\begin{aligned}
 |F(u, v)|^2 = & |R(u, v)|^2 + \sum_{i=1}^n |T_i(u, v)|^2 + 2 \sum_{i=1}^n |T_i(u, v)| |R(u, v)| \cos[\Phi_n(u, v) - \Phi_r(u, v) \\
 & - ux_i - vy_i - 2vy_0] + 2 \sum_{i=1}^n \sum_{k=1, k \neq i}^n |T_i(u, v)| |T_k(u, v)| \cos[\Phi_n(u, v) - \Phi_{ik}(u, v) \\
 & - ux_i + ux_k - vy_i + vy_k]
 \end{aligned} \quad (3.3)$$

By subtracting the reference only power spectra and the input scene only power spectra, we get the modified JPS for multi-object input scene as given by

$$\begin{aligned}
 P(u, v) = & |F(u, v)|^2 - |R(u, v)|^2 - \sum_{i=1}^n |T_i(u, v)|^2 \\
 = & \sum_{i=1}^n |R(u, v)| |T_i(u, v)| \exp[j(\Phi_r(u, v) - \Phi_n(u, v) + ux_i + v(y_0 + y_i))] \\
 & + \sum_{i=1}^n |R(u, v)| |T_i(u, v)| \exp[-j(\Phi_r(u, v) - \Phi_n(u, v) + ux_i + v(y_0 + y_i))]
 \end{aligned} \quad (3.4)$$

Inverse Fourier transform of Eq. (2.10) gives the correlation output for the multi-object input scene as expressed by

$$\begin{aligned}
 g(x', y') = & \sum_{i=1}^n r(-x' - x_i, -y' - y_i - 2y_0) \otimes t_i^*(-x', -y') \\
 & + \sum_{i=1}^n r^*(x' - x_i, y' - y_i + 2y_0) \otimes t_i(x', y')
 \end{aligned} \quad (3.5)$$

In Eq. (2.11), again there are only cross-correlation terms between the reference and target images only. The Fourier plane image subtraction technique eliminates the zero-order term and other false alarms generated by the cross-correlation among different objects in the input scene.

3.2.1 Simulation Results

To analyze the performance of unnormalized intensity varying targets, a binary character 'E' of English Alphabet has been taken as the reference image. The size of the character is 32×32 pixels and it is placed in a joint image of size 256×256 pixels. The joint image contains multiple objects (target and non-targets) as shown in Fig. 3.1(a). Two non targets, 'H' and 'T', of four and seven times illumination intensity, respectively, and two targets, 'E' of similar and two times illumination intensity than the reference image, 'E' have been considered. The simulations are performed using FFT2 routine of MATLAB software and the outputs are plotted using the 3-D plotting routine.

The joint image has been processed to find the correlation output of Fig 3.1 (b). It shows four cross-correlation peaks of different heights for the targets and non-targets. As the intensity of 'H' and 'T' are stronger than the targets, the cross correlation peaks are found to be higher than the auto correlation peaks produced by the targets. So unnormalized recognition leads to false alarms.

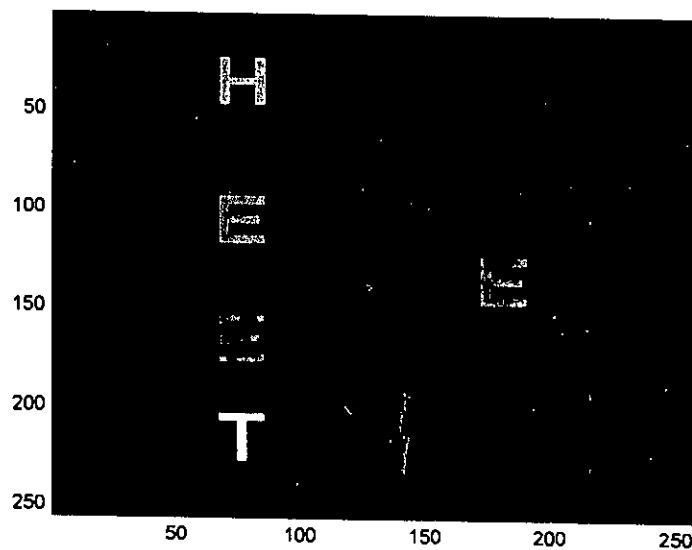


Fig. 3.1(a) Input joint image with multiple targets and non-targets

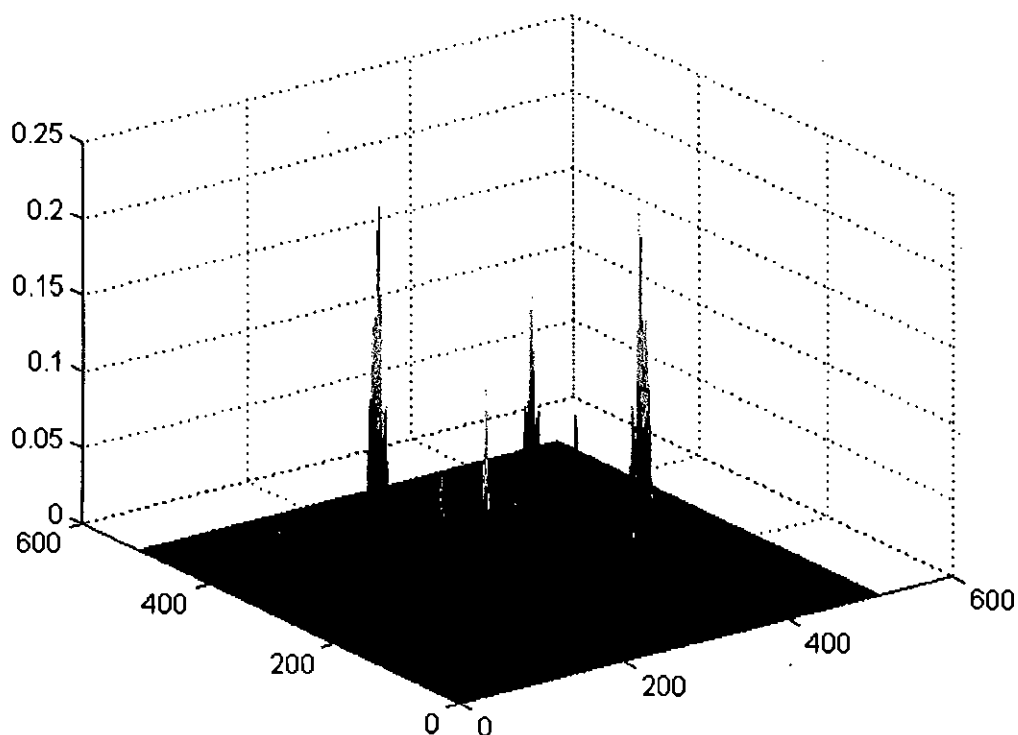


Fig. 3.1(b) Unnormalized correlation output for joint image with varying illumination

Again, four targets are considered as shown in Fig 3.2 (a) with four, two, one and seven times illumination intensity than the reference image is taken. Fig 3.2 (b) gives the correlation output where there are four pairs of peaks of different amplitudes. Accurate recognition on the quantity of targets cannot be achieved from this correlation output which is misleading.

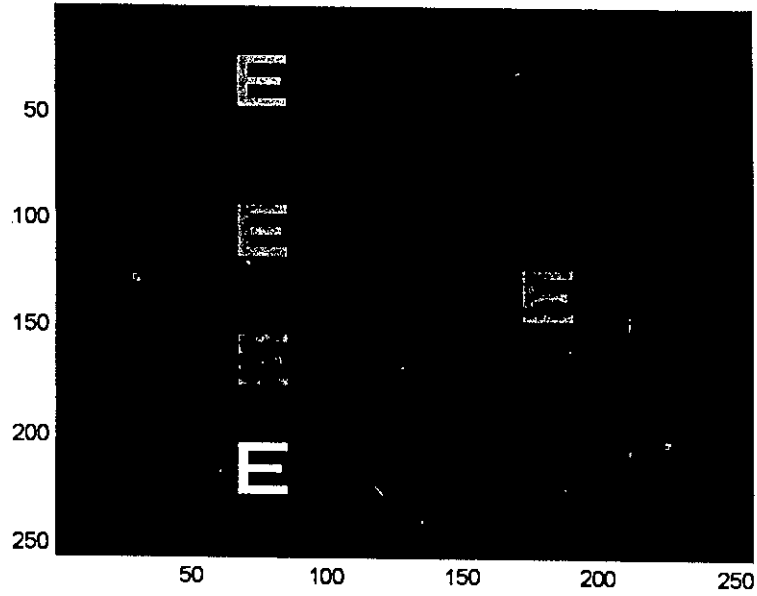


Fig. 3.2(a) Input joint image with multiple targets with varying illumination

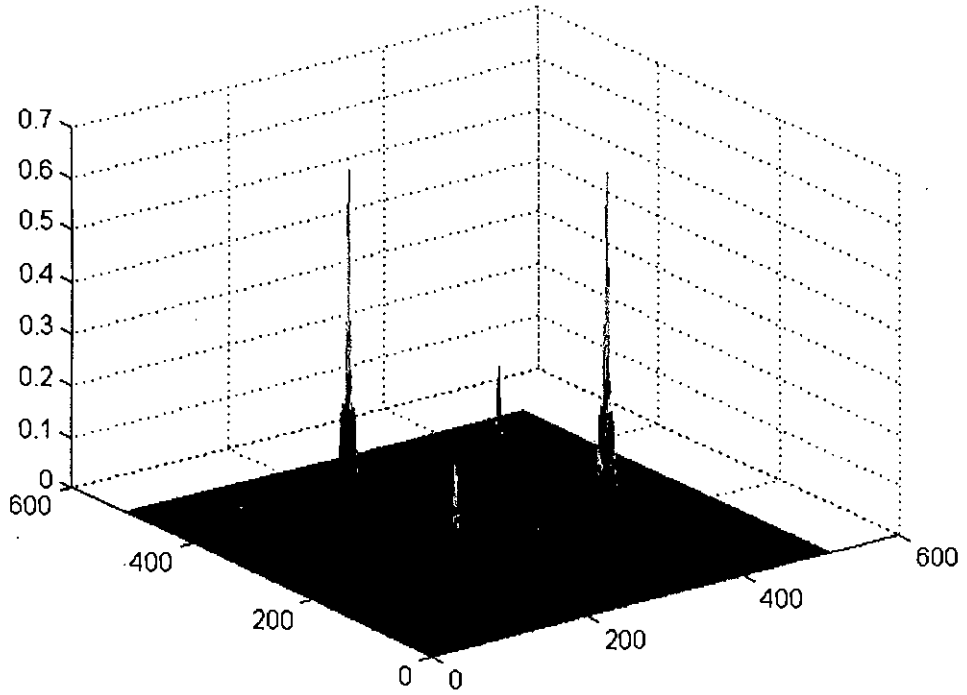


Fig. 3.2(b) Correlation output for four targets with varying illumination

3.3 Normalized Intensity Varying Multi-target Detection

3.3.1 Normalized Correlation

Let If $t(x,y)$ and $r(x,y)$ are the target and the reference images respectively, then output of an optical linear correlator is computed as

$$C(x', y') = \left| \iint t(x+x', y+y')s(x, y)r(x, y) dx dy \right|^2 \quad (3.6)$$

where,

$$s(x, y) = \begin{cases} 1 & x, y \in \text{support of } r(x, y) \\ 0 & \text{otherwise} \end{cases}$$

and

$$s(x, y) r(x, y) = r(x, y)$$

Here $s(x, y)$ defines the region of $r(x, y)$ to be compared to $t(x, y)$.

Application of Cauchy-Schwarz inequality to the above equation gives

$$C(x', y') \leq \iint |t(x+x', y+y')s(x, y)|^2 dx dy \iint |r(x, y)|^2 dx dy \quad (3.7)$$

$$\begin{aligned} \Rightarrow & \left| \iint t(x+x', y+y')s(x, y)r(x, y) dx dy \right|^2 \\ & \leq \iint |t(x+x', y+y')s(x, y)|^2 dx dy \iint |r(x, y)|^2 dx dy \end{aligned}$$

$$\begin{aligned} \Rightarrow & \left| \iint t(x+x', y+y')r(x, y) dx dy \right|^2 \\ & \leq \iint |t(x+x', y+y')s(x, y)|^2 dx dy \iint |r(x, y)|^2 dx dy \end{aligned}$$

$$\Rightarrow \frac{\left| \iint t(x+x', y+y')r(x, y) dx dy \right|^2}{\iint |t(x+x', y+y')s(x, y)|^2 dx dy \iint |r(x, y)|^2 dx dy} \leq 1$$

The normalized correlation is thus defined as:

$$N(x', y') = \frac{\left| \iint t(x+x', y+y')r(x, y)dx dy \right|^2}{\iint |t(x+x', y+y')s(x, y)|^2 dx dy \iint |r(x, y)|^2 dx dy} \leq 1 \quad (3.8)$$

With equality if and only if,

$$r(x, y) = k \cdot t(x, y)s(x, y), \quad (3.9)$$

where k is a constant. So we see from the above two equations that normalized correlation reaches its maximum value 1 if and only if $t(x, y)$ and $r(x, y)$ are matched. Otherwise, a normalized value less than 1 is obtained. Values closer to 1 represent a better match. It is the factor k that contributes to intensity invariance.

Since, $t(x, y)$, $r(x, y)$ and $s(x, y)$ are nonnegative in image recognition and $s^2(x, y) = s(x, y)$ then,

$$\begin{aligned} N(x', y') &= \frac{\left[\iint t(x+x', y+y')r(x, y)dx dy \right]^2}{\iint t^2(x+x', y+y')s(x, y)dx dy \iint r^2(x, y)dx dy} \\ &= \frac{1}{c} \frac{[t(x', y') \otimes r(x', y')]^2}{t^2(x', y') \otimes s(x', y')} \end{aligned} \quad (3.10)$$

where \otimes denotes the cross-correlation operation and

$$c = \iint r^2(x, y)dx dy \quad (3.11)$$

Here c is a constant. Note that c can be calculated in advance simply by summing all pixel values of the reference. The normalized correlation thus becomes the ratio of two cross correlations. The pointwise division can be performed using a computer while the two cross-correlations can be obtained in real time using JTC in parallel.

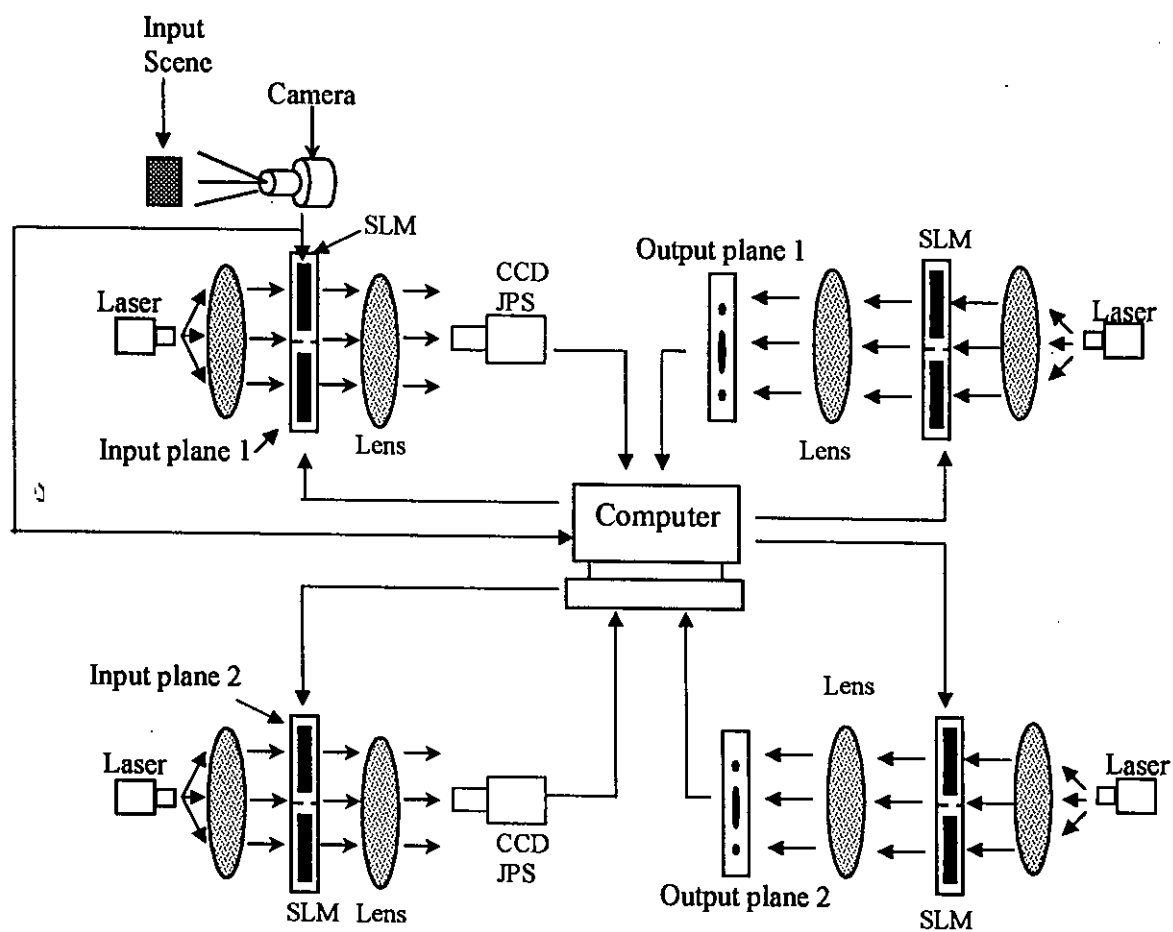


Fig. 3.3(a) Architecture of the proposed normalized joint transform correlator technique

3.3.2 Theoretical Analysis

Two input planes each consisting of two inputs will be employed. The first input plane displays the reference image $r(x,y)$ and target image $t(x,y)$ while the second input plane shows the square of the target image $t^2(x,y)$ and support of the reference $s(x,y)$. Both of the input planes are illustrated in the Fig 3.3(b). The first input plane can be considered as the combination of two joint images described as

$$f_1(x, y) = t(x + a, y - b) + r(x - a, y + b) \quad (3.12)$$

And the second input planes can be considered as the combination of two joint images in expressed as

$$f_2(x, y) = t^2(x + a, y - b) + s(x - a, y + b) \quad (3.13)$$

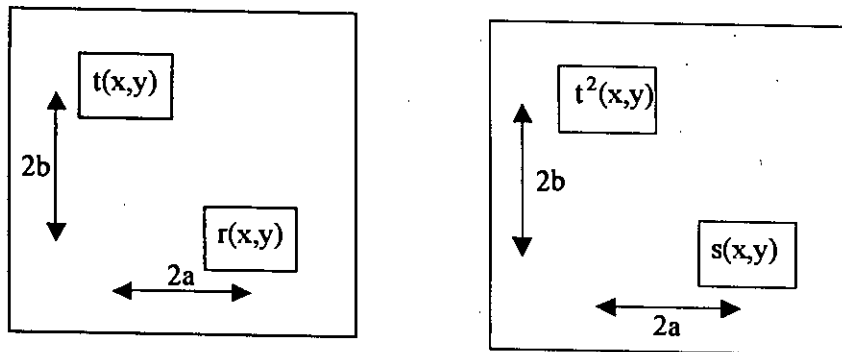


Fig. 3.3(b) First and second input planes with the joint images

By using a lens let $f_1(x, y)$ be Fourier transformed to yield

$$F_1(u, v) = |R(u, v)| \exp[j\Phi_r(u, v) - jua + jvb] + |T(u, v)| \exp[j\Phi_t(u, v) + jua - jvb]$$

where $R(u, v)$ and $T(u, v)$ are the amplitudes, $\Phi_r(u, v)$ and $\Phi_t(u, v)$ are the phases of the Fourier transforms of $r(x, y)$ and $t(x, y)$, respectively; u and v are mutually independent frequency domain variables scaled by a factor of $\frac{2\pi}{\lambda}$, λ is the wavelength

of collimating light, f is the focal length of the lens. The complex light distribution produced in the back focal plane of the lens, called the JPS, is then detected by a square-law device such as a CCD array. The JPS is given by

$$\begin{aligned}
 |F_1(u, v)|^2 &= F_1(u, v) \cdot F_1^*(u, v) \\
 &= [|R(u, v)| \exp(j\Phi_r(u, v) - jua + jvb) + |T(u, v)| \exp(j\Phi_t(u, v) + jua - jvb)] \\
 &\quad [|R(u, v)| \exp(-j\Phi_r(u, v) + jua - jvb) + |T(u, v)| \exp(-j\Phi_t(u, v) - jua + jvb)] \\
 &= |R(u, v)|^2 + |T(u, v)|^2 + |R(u, v)||T(u, v)| \times \exp[j\Phi_r(u, v) - j\Phi_t(u, v) - j2ua + j2vb] + \\
 &\quad |T(u, v)||R(u, v)| \times \exp[j\Phi_t(u, v) - j\Phi_r(u, v) + j2ua - j2vb]
 \end{aligned} \tag{3.14}$$

If the zero-order term of the joint power spectrum is eliminated then the on-axis correlation distribution can be avoided. Since the zero-order correlation are derived from the individual power spectrum of $r(x, y)$ and $t(x, y)$, these power spectrum can be eliminated from the joint power spectrum by the use of computer. Fourier plane image subtraction technique is employed. After subtracting these two terms the JPS for single object input scene becomes

$$\begin{aligned}
 F_1'(u, v) &= |F_1(u, v)|^2 - |R(u, v)|^2 - |T(u, v)|^2 \\
 &= |R(u, v)||T(u, v)| \times \exp[j\Phi_r(u, v) - j\Phi_t(u, v) - j2ua + j2vb] + \\
 &\quad |T(u, v)||R(u, v)| \times \exp[j\Phi_t(u, v) - j\Phi_r(u, v) + j2ua - j2vb]
 \end{aligned} \tag{3.15}$$

Now inverse Fourier transform of the above equation produces the final correlation output as

$$f_1'(x, y) = r(x, y) \otimes t(x, y) * \delta(x + 2a, y - 2b) + t(x, y) \otimes r(x, y) * \delta(x - 2a, y + 2b) \tag{3.16}$$

Similarly performing Fourier transform on the second input plane by a lens, Fourier plane image subtraction technique on the JPS and finally inverse Fourier transform yields the following output plane correlation distribution

$$f_2'(x, y) = s(x, y) \otimes t^2(x, y) * \delta(x + 2a, y - 2b) + t^2(x, y) \otimes s(x, y) * \delta(x - 2a, y + 2b) \quad (3.17)$$

The output plane correlation distribution of both the input planes are shown in Fig. 3.3(c) as follows

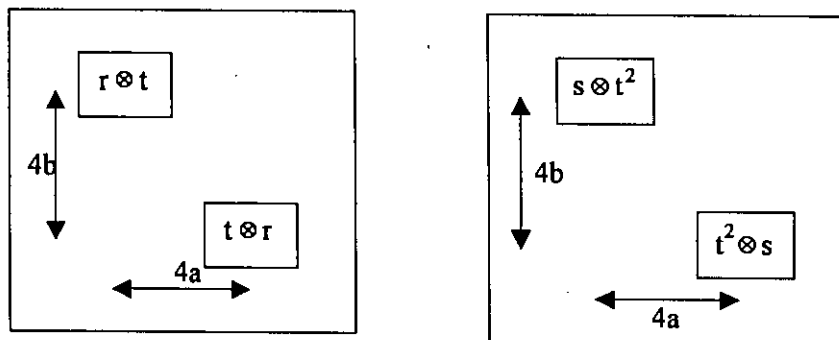


Fig. 3.3(c) Output planes with correlation distribution

Squaring the first output plane and then pointwise division can be performed using a computer which will yield to give normalized correlation. Extraction of the desired terms is easy as they are the only ones left after the Fourier plane image subtraction technique is employed. So false peaks are eliminated and fewer correlation terms are produced at the output planes which results an increase in detection efficiency.

3.3.3 Simulation Results

To analyze the performance of normalized intensity varying targets, a binary character 'E' of English Alphabet has been taken as the reference image. The size of the character is 32×32 pixels and it is placed in a joint image of size 256×256 pixels. The joint image contains multiple objects (target and non-targets) as shown in Fig. 3.4(a). Two non targets, 'H' and 'T', of four and seven times illumination intensity, respectively, and two targets, 'E' of similar and two times illumination intensity than the reference

image, 'E' have been considered. The simulations are performed using FFT2 routine of MATLAB software and the outputs are plotted using the 3-D plotting routine.

The input plane distribution is shown in Fig 3.4(b) and Fig 3.4(c). They are of 512X512 pixel each. Here in the first input plane target and reference is taken and in the second input plane the square of the target and the support of the reference is employed. Two out plane distributions are shown in Fig 3.4(d) and Fig 3.4(e). After the image has been processed, the final normalized correlation output is shown in Fig 3.4(f).

The correlation output shows four cross-correlation peaks for the targets and non-targets. Two peaks are of same height and represent the targets. Although the intensity of 'H' and 'T' are stronger than the targets, the cross correlation peaks are found to be much lower than the auto correlation peaks produced by the targets. So normalized recognition leads to proper detection of targets under different illumination.

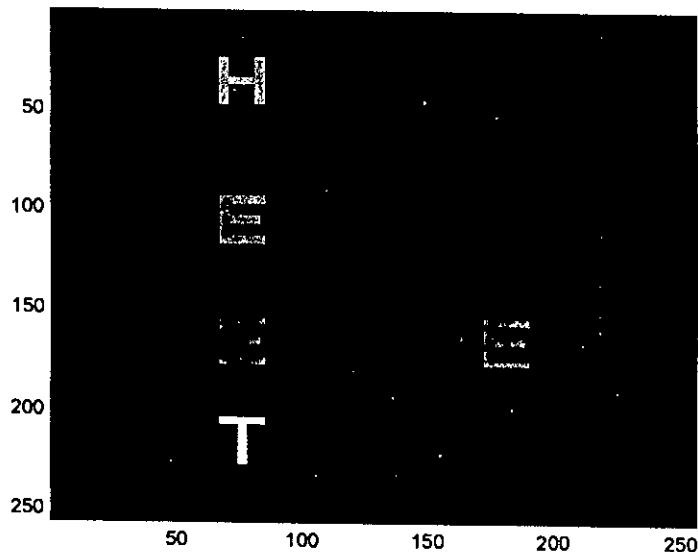


Fig. 3.4(a) Input joint image with multiple targets and non-targets

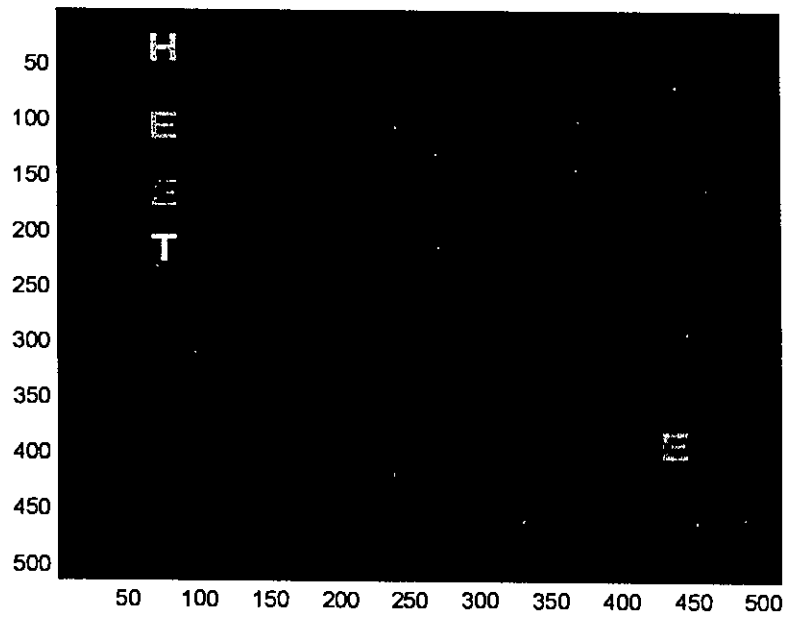


Fig. 3.4(b) First input plane distribution containing the reference and input joint image

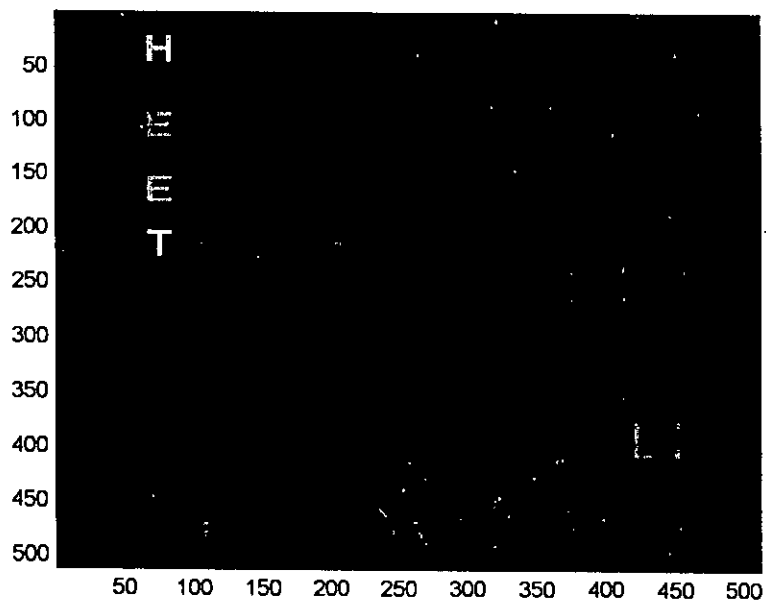


Fig. 3.4(c) Second input plane distribution containing the square of the input image and the support of the reference

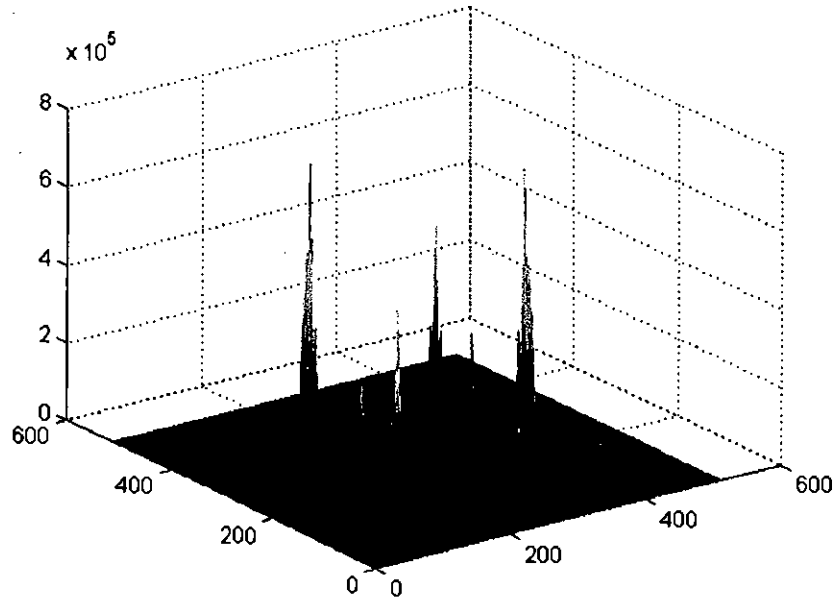


Fig. 3.4(d) First correlation output plane distribution

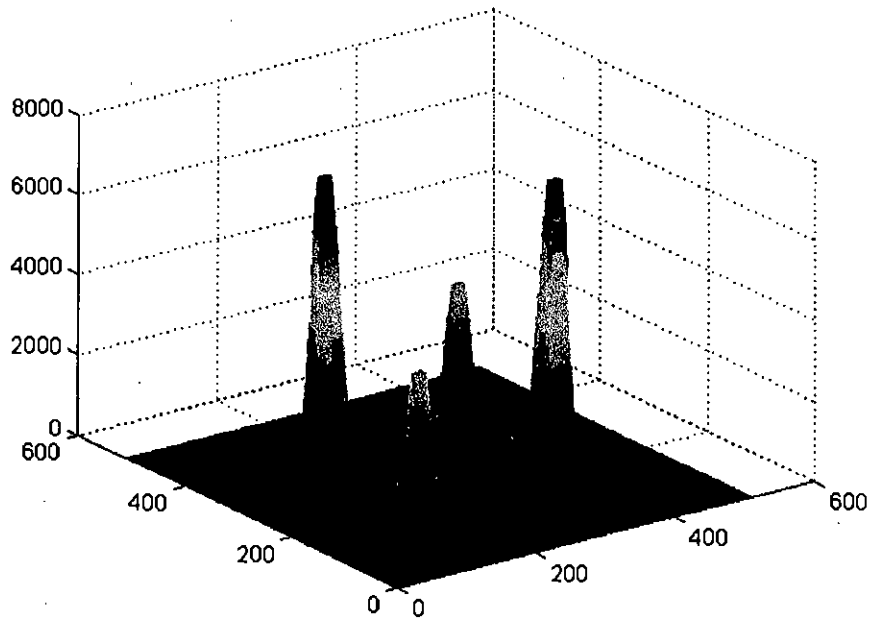


Fig. 3.4(e) Second correlation output plane distribution

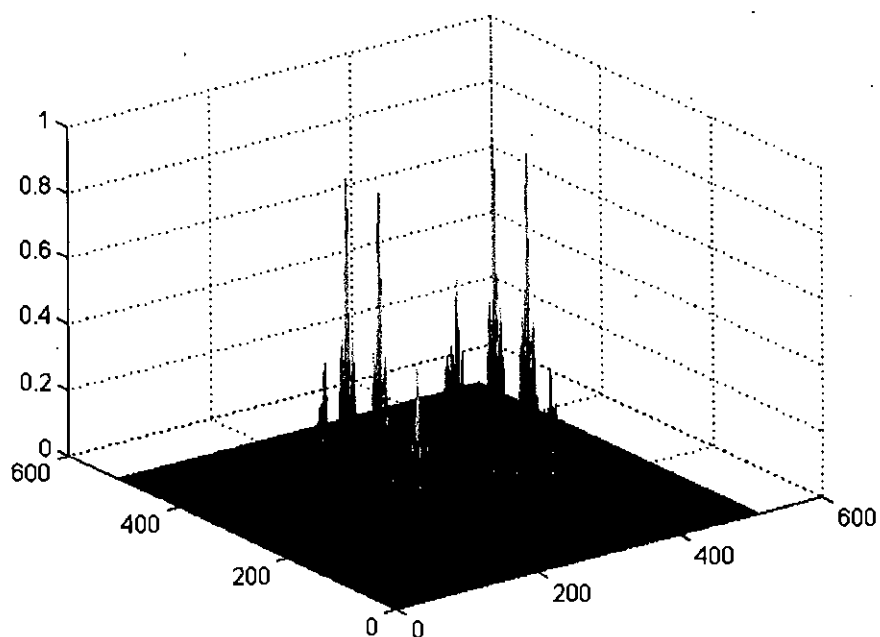


Fig. 3.4(f) Normalized correlation output for joint image with varying illumination

Again, four targets are considered as shown in Fig 3.5 (a) with four, two, one and seven times illumination intensity than the reference image is taken. Fig 3.5 (b) gives the correlation output where there are four pairs of peaks of same amplitudes. Accurate recognition on the quantity of targets can be achieved from this correlation output whether they are of different illumination intensity or not.

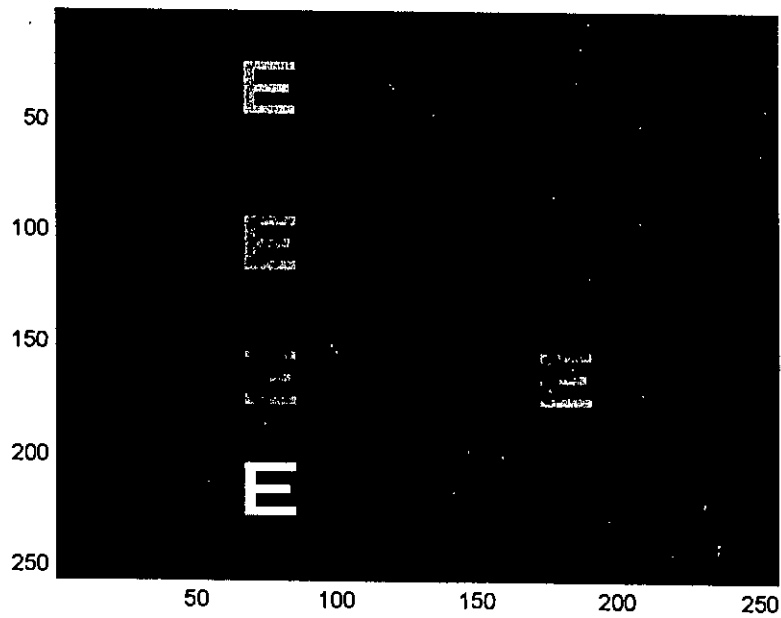


Fig. 3.5(a) Input joint image with multiple targets with varying illumination

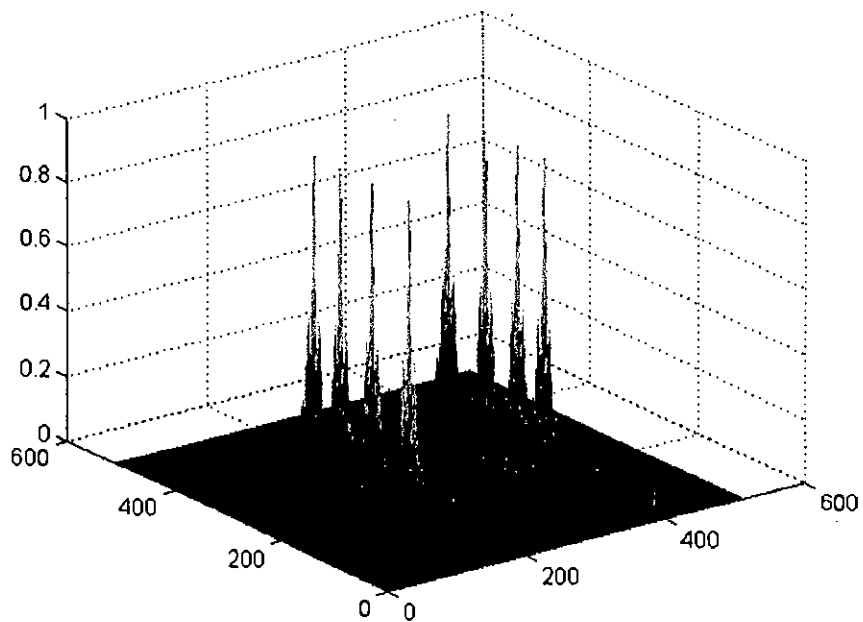


Fig. 3.5(b) Normalized correlation output for four targets with varying illumination

3.4 Post Processing Technique

3.4.1 Theoretical Analysis

In the thesis work, a post-processing technique has been developed to increase the discrimination ratio. Here, the normalized correlation output $O(x,y)$ is first squared by a CCD and is then divided by the negative exponential of the squared correlation output as expressed by

$$O_p(x,y) = \frac{|O(x,y)|^2}{\exp[-O(x,y)^2]} \quad (3.18)$$

where $O(x,y)$ is the normalized actual correlation output and $O_p(x,y)$ is the output after post-processing.

The algorithm of developing this post processing technique is based on the fact that to enhance the discrimination capability between targets and non-targets, sharper delta like peaks of the targets is required and the non-target peaks needs to be diminished. So by using the nature of a negative exponential function this may be achieved.

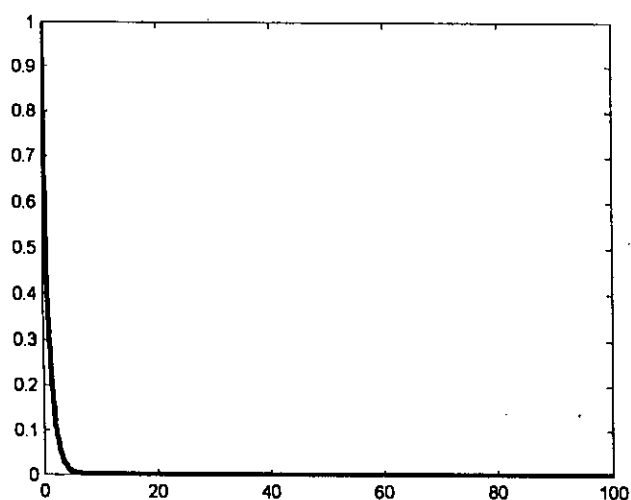


Fig. 3.6 Negative exponential function

Here by dividing the squared normalized correlation output by the negative exponential of the squared correlation output we will achieve good discrimination capability. Here higher amplitude terms will increase in amplitude as they are divided by smaller values and the smaller amplitude terms of the output will be diminished as they are divided by larger values. Applying this post processing to the correlation output obtained before proves the effectiveness of the proposed method.

3.4.1 Simulation Results

To analyze the performance of the post processing technique, it is applied to the correlation outputs as shown in Fig 3.4(a) and 3.5(b). Fig. 3.7(a) and 3.7(b) show the after effect of post-processing technique of the correlation outputs respectively.

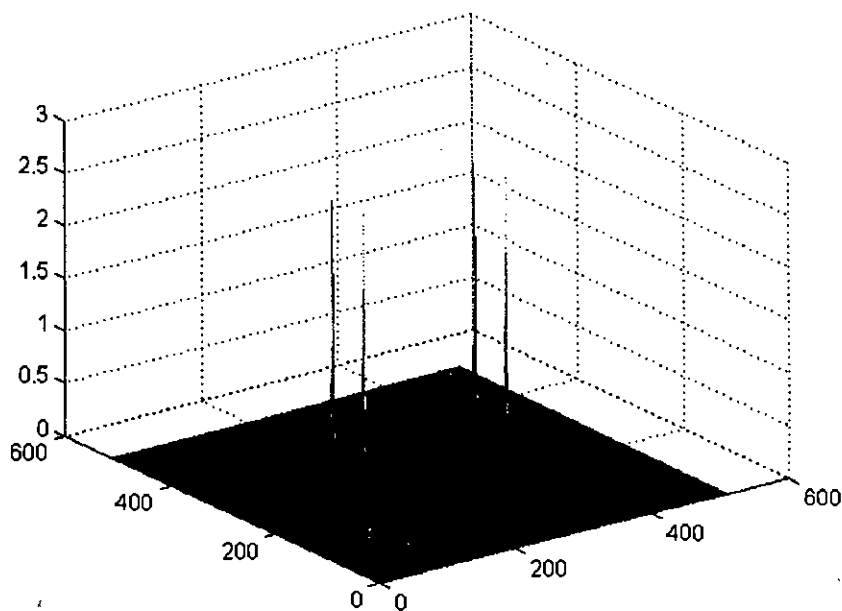


Fig. 3.7(a) Two delta like peaks represents the two targets and the non targets peaks are diminished significantly.

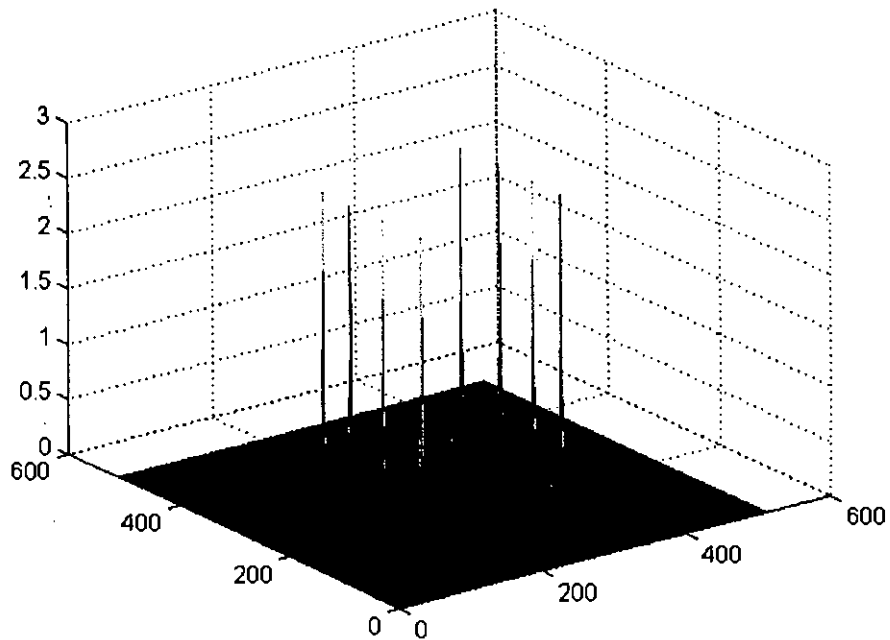


Fig 3.7 (b) Four delta like peaks represent the four illumination varying targets.

3.5.1 Performance Evaluation of the Proposed Scheme

Four criteria may be used for evaluation of the performance of the proposed scheme. They are normalized correlation peak intensity (CPI), peak to clutter ratio (PCR), the full width at half maximum (FWHM) power point and the peak to side lobe ratio (PSR).

Normalized correlation peak intensity is the normalization of all the peaks obtained based on the highest peak intensity strength. It provides the comparison of all the output peaks with the maximum one.

Peak to clutter ratio can be defined as the ratio of the minimum target peak to the maximum non-target peak in the correlation output distribution. Higher the value of the PCR, better the discrimination ratio between targets and non-targets.

Full width at maximum power point represents the width of the output peaks at the half point of the peaks. Smaller value of the FWHM means that the peaks are more sharper and more delta like.

Peak to side lobe ratio is another performance criteria which can be defined as the ratio of the target peak to the side lobe peak. We want the side lobe to be as small as possible because they may lead to false target detection. So higher the PSR, better the correlation output in detecting the targets from the input scene.

Comparative performance of classical JTC technique with normalized JTC technique in respect of CPI is given in Table 3.1. We are taking four targets "E" with the following intensity variation in the input scene. There is a proportional decrease in CPI with intensity for classical JTC where for normalized JTC the CPI is the same. So if we do not do normalization we cannot accurately detect the number of targets from the decreasing output of the classical JTC. But as the normalized JTC gives the same intensity strength at the correlation output for all the targets, the possibility of false alarms is zero.

Table 3.1: Comparative analysis of classical JTC and normalized JTC where the input plane contains only targets

Intensity Strength	Normalized CPI with Classical JTC	Normalized CPI with Normalized JTC
7	1.00	1.00
4	0.725	1.00
2	0.25	1.00
1	0.0525	1.00

If we take the input scene distribution where there are two non-targets "H" and "T" and two targets "E" of varying intensity and we do a comparison with the classical JTC and normalized JTC without and with post processing we find the analysis as given in Table 3.2.

Table 3.2: Comparative study of input image containing targets and non-targets.

Performance Criteria	Classical JTC	Normalized JTC without Post processing	Normalized JTC with post processing
Normalized CPI	1.00, 0.36	1.00, 1.00	1.00, 1.00
PCR	0.234	1.917	7.612
FWHM	6	3	1.00
PSR	1.42	2.65	7.94

From the table, we can see that normalized JTC gives the same CPI where the classical JTC produces different CPI for different targets. This will arise misleading target detection. The PCR and PSR is much lower and the FWHM is higher for the classical JTC which is not desirable.

From the comparative analysis of normalized JTC with and without post processing, we can see that the post processing gives better results in respect of PCR, FWHM and PSR. The FWHM decreases to '1', which means that sharp delta like peaks are produced. The PCR and PSR are also high enough to avoid any false target detection.

Furthermore, if we apply the post processing technique to the input scene distribution where only four illumination varying targets are present we can see that it also gives better performance in respect to FWHM and PSR as shown in Table 3.3. The PCR cannot be calculated here because there are no targets present in the input scene.

Table 3.3: Applying the post processing technique to the input scene with only targets but illumination varying

Performance Criteria	Normalized JTC without Post processing	Normalized JTC With post processing
Normalized CPI	1.00, 1.00, 1.00, 1.00	1.00, 1.00, 1.00, 1.00
FWHM	4	1.00
PSR	1.95	7.94

From the above analysis we can see that the application of the post processing technique to the correlation output gives better performance and increases the detection efficiency.

3.5.2 Comparative Analysis

For a comparative study of the normalized joint transform correlator with the morphological correlation based joint transform correlator, we analyzed the time required for detection of binary images with the input scene containing targets and non-targets. Both techniques were run using the MATLAB 5.3 and a 2.4 GHz Pentium processor. The following table gives the results.

Table 3.4: Comparative analysis of normalized JTC with the morphological JTC

Detection Method	Detection time (sec)
Normalized JTC without post processing	3.0780
Normalized JTC with post processing	3.2820
Morphological based JTC	6.7370

From the study, we can see that by introducing the post processing, time required to detect the targets increased a little bit but it is still less than that of the morphological based joint transform correlator. So in terms of detection time, the normalized JTC is faster.

3.6 Detection of Gray Scale Image

3.6.1 Input Scene Containing Only Targets

We take the well known image “Lena” in evaluating performance of the proposed scheme. The input scene contains similar, 60% brighter and 60 % darker intensity of the reference Lena taken. The size of the lena image is 56X64 pixel and it is placed in a joint image of 256X256 pixels. So the input scene has illumination varying gray scale images of only targets. Both of the input planes are of 512X512 pixels.

The correlation output gives three pairs of peaks of almost equal amplitude. The post processing gives better output by providing sharper delta like peaks. So accurate recognition on the quantity of targets can be achieved from this correlation output whether the images are gray scale and varying illumination intensity.

Fig. 3.8(a) gives the image “Lena” which is taken for testing the proposed scheme. Fig. 3.8(b) gives the input scene distribution of varying illumination of “Lena” and the reference. Fig. 3.8(c) and Fig. 3.8(d) gives the two output planes obtained and Fig. 3.8(e) gives the normalized correlation output without the post processing. Finally Fig. 3.8(f) gives the normalized correlation output with post processing technique.



Fig. 3.8(a) Gray scale image of Lena

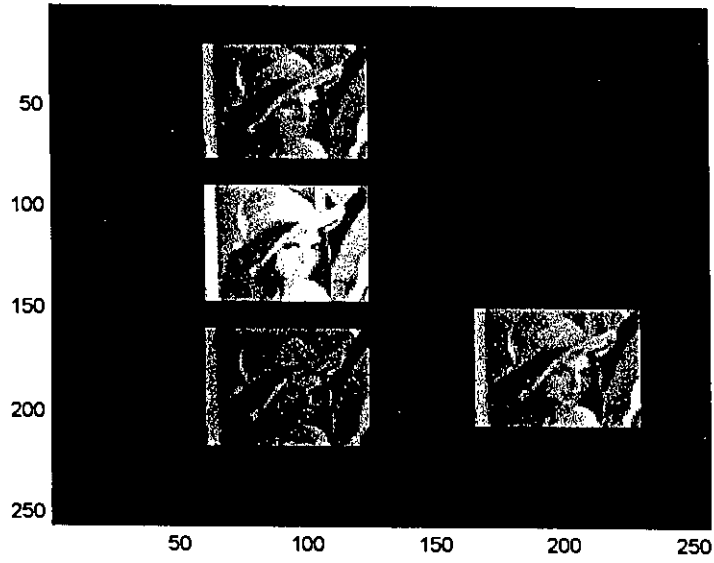


Fig. 3.8(b) Input joint image with multiple targets with varying illumination and the reference.

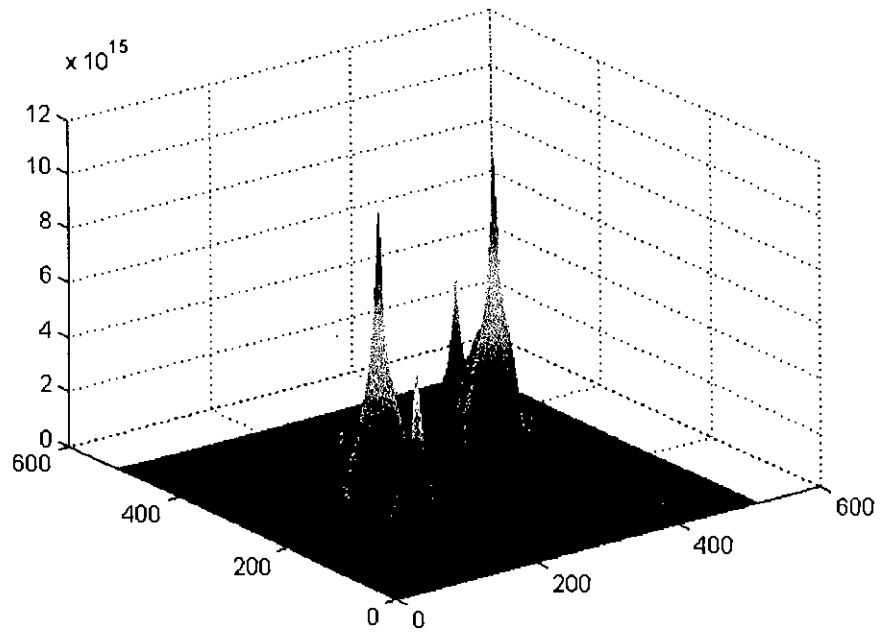


Fig. 3.8(c) First correlation output plane distribution

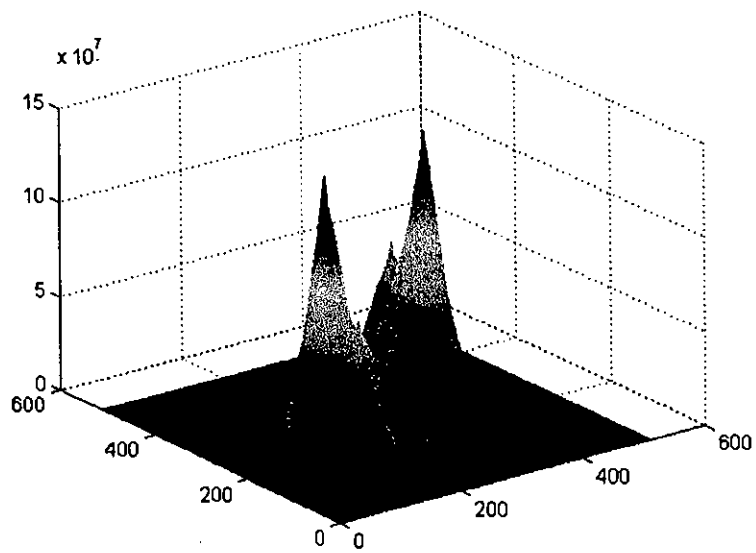


Fig. 3.8(d) Second correlation output plane distribution

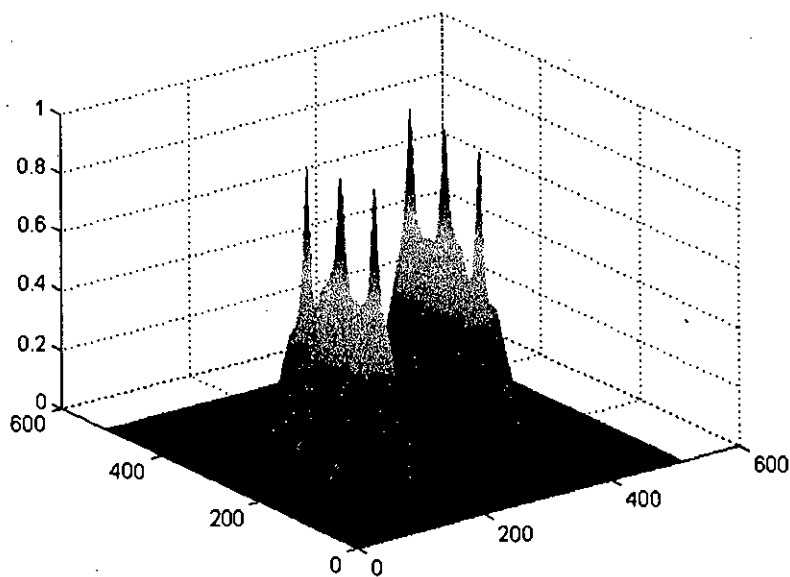


Fig. 3.8 (e) Normalized correlation output without post processing

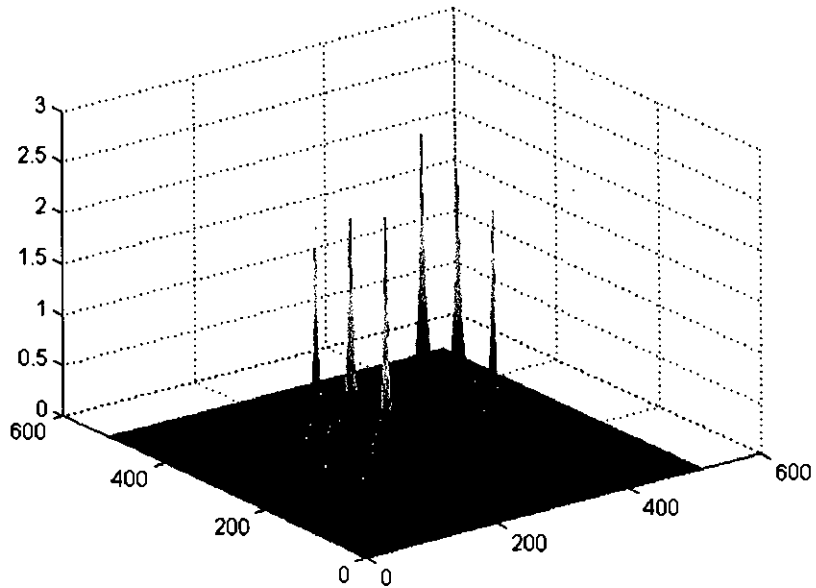


Fig. 3.8 (f) Normalized correlation output with post processing

3.6.2 Performance Evaluation

The post processing technique improves the normalized correlation output significantly. The FWHM is greatly reduced as it produces sharper peaks. Although the CPI for the targets decreases when the post processing technique is applied, but it is negligible and will not affect the detection of targets. The PSR also almost doubles and increases the detection efficiency. Table 3.4 gives the evaluation in detail.

Table 3.5: Performance analysis in the detection of grayscale image lena

Performance Criteria	Normalized JTC without Post processing	Normalized JTC With post processing
Normalized CPI	1.00,0.9841,0.9583	1.00,0.934, 0.846
FWHM	471	5
PSR	1.29	2.49

3.6.3 Input Scene Containing Targets and Non-Targets

We take the gray scale image of two cars, which are very close in resemblance. The target is shown in Fig 3.9(a) and the non-target is shown in Fig. 3.9(b). The targets also vary in illumination. The input scene contains the non-target, 60% brighter and 60 % darker intensity of the reference car taken, which is given in Fig 3.9(c). The size of the target and non-target cars is 34X64 pixel and it is placed in a joint image of 256X256 pixels. So the input scene has illumination varying gray scale images of targets and non-targets. Both of the input planes are taken of 512X512 pixels.

The correlation output gives three pairs of peaks as given in Fig 3.9(d). Two pairs of peaks are almost equal in amplitude and we can declare them as targets. But third pair of peak is a little bit smaller in amplitude but if the threshold level is not set properly, we can misinterpret it as a target also. But after the post processing technique, which is shown in Fig 3.9(e), we get sharper delta like peaks for the targets and the amplitude of the non-target pair of peaks decreases significantly which improves the possibility of accurate recognition of targets. There is no possibility of considering this as a target. Hence the post processing technique increases the discrimination ratio between targets and non-targets significantly.

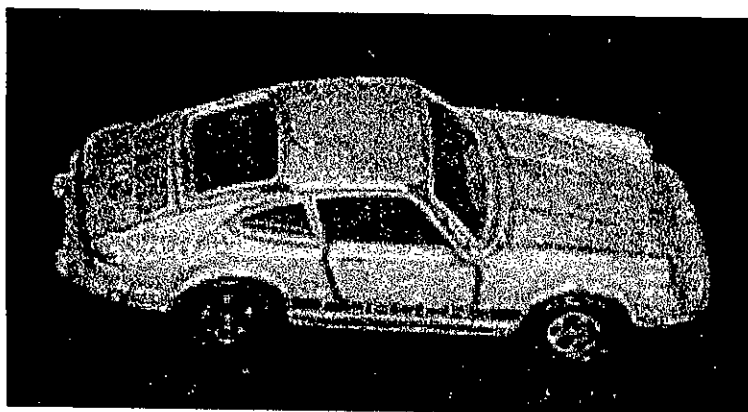


Fig. 3.9 (a) Image of the target car

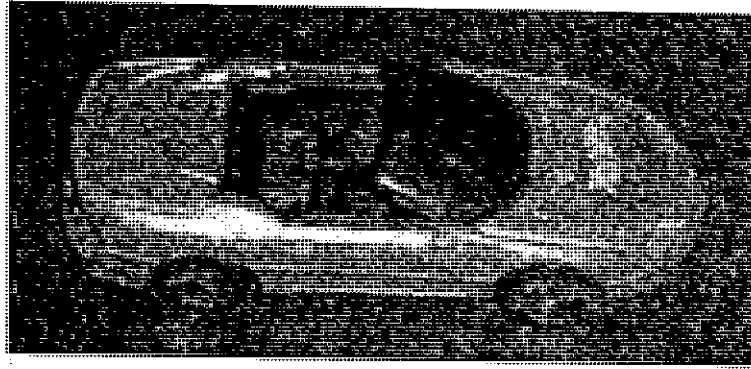


Fig. 3.9 (b) Image of the non-target car

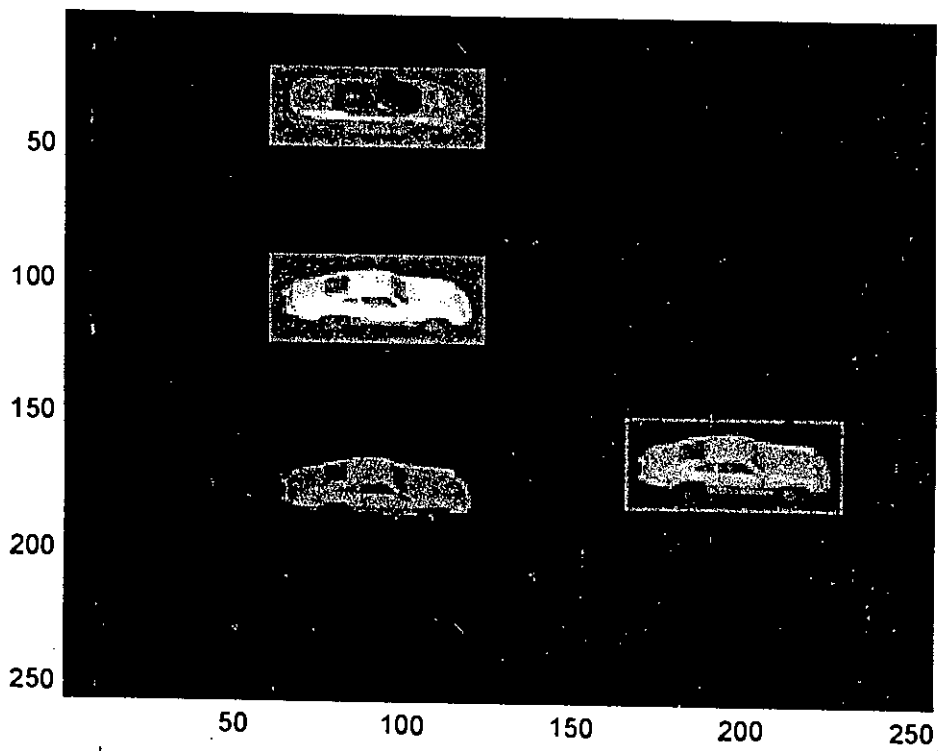


Fig. 3.9(c) Input joint image with multiple targets and non-target with varying illumination and the reference.

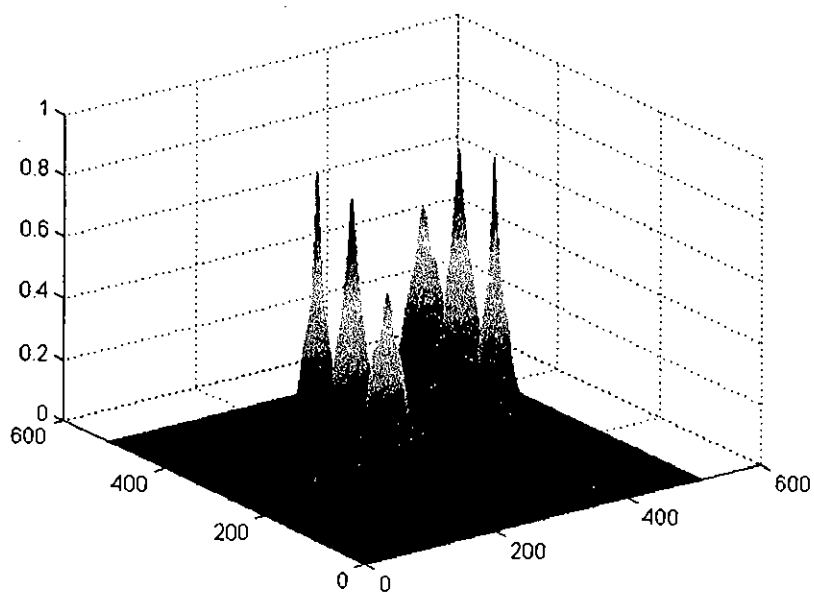


Fig. 3.9 (d) Normalized correlation output without post processing

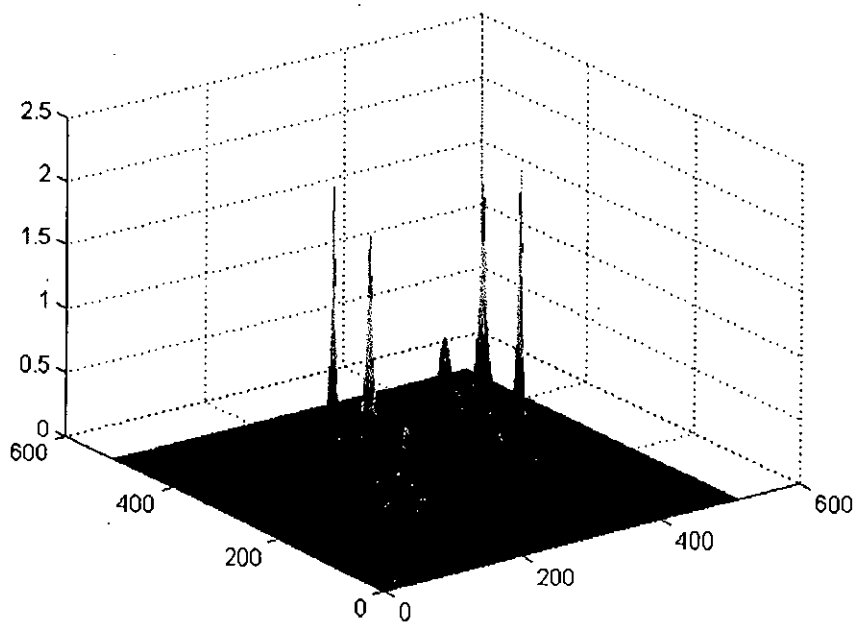


Fig. 3.9 (e) Normalized correlation output with post processing

3.6.4 Performance Evaluation

The post processing technique improves the normalized correlation output significantly. The FWHM is greatly reduced as it produces sharper peaks. Here from the values of normalized CPI without post processing we see that the difference between the amplitudes of targets and non-targets is not much. So false target detection is possible with not proper threshold setting. But after the post processing the value reaches below 0.5 and we can certainly detect it as a non-target.

Table 3.6: Performance analysis in the detection of grayscale image of targets and non-targets

Performance Criteria	Normalized JTC without Post processing	Normalized JTC With post processing
Normalized CPI	0.9630, 0.9341, 0.7682	1.00, 0.89, 0.42
PCR	1.215	2.15
FWHM	165	4
PSR	1.418	3.20

3.6.5 Comparative Analysis

For a comparative study of the normalized joint transform correlator with the morphological correlation based joint transform correlator, we analyzed the time required for detection of gray scale images with the input scene containing Lena. Both techniques were run using the MATLAB 5.3 and a 2.4 GHz Pentium processor. The following table gives the results.

Table 3.7: Comparative analysis of normalized JTC with the morphological JTC

Detection Method	Detection time (sec)
Normalized JTC without post processing	3.4220
Normalized JTC with post processing	3.7350
Morphological based JTC	7.0256

From the study, we can see that the NJTC is faster than the morphological based correlator when detecting gray level images.

3.7 Detection of Targets Under Noisy Conditions

3.7.1 Noisy Binary Image detection

3.7.1.1 Binary Image Containing Only Targets

To investigate the noise robustness of the system, additive gaussian white noise is added in the input scene. Fig 3.10(a) shows the joint image with an additive white noise of 0db in the input scene. Fig 3.10(b) shows the corresponding normalized correlation output of Fig 3.10(a).

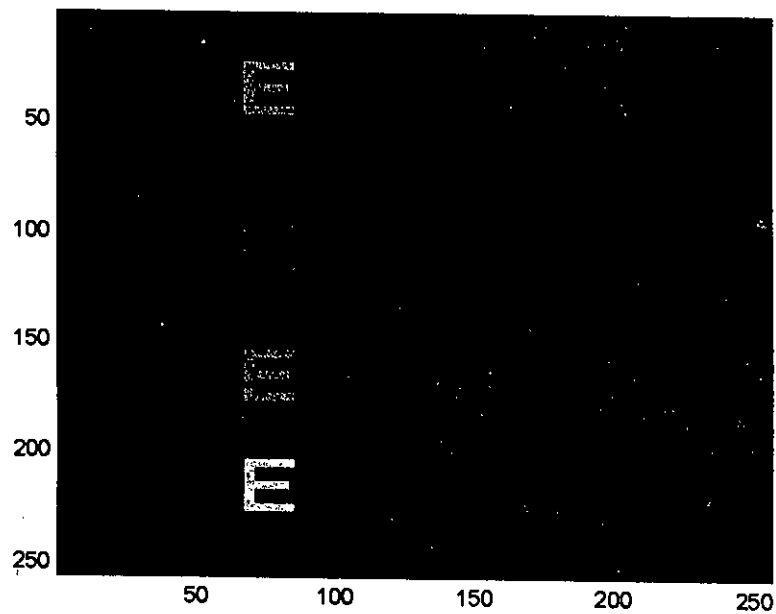


Fig. 3.10 (a) Joint image with an additive white noise of 0db

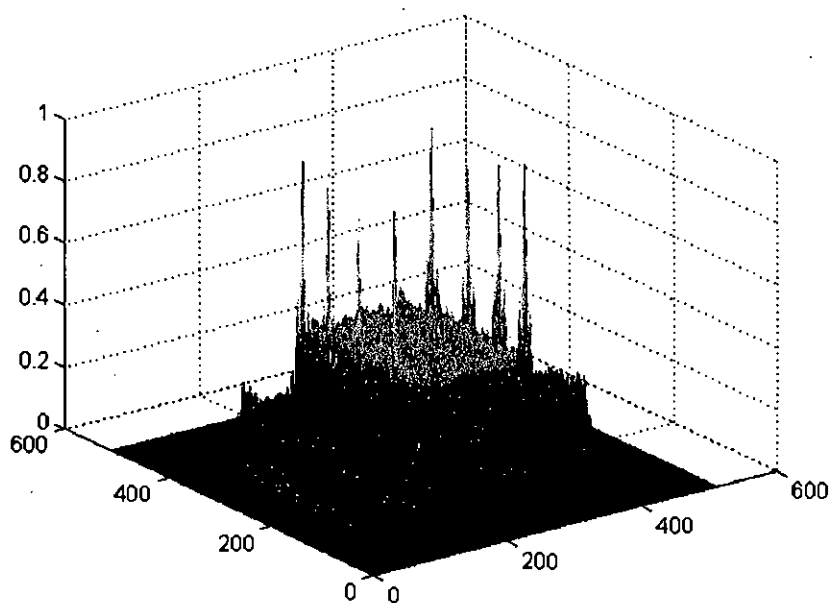


Fig. 3.10 (b) Corresponding correlation output an additive white noise of 0db. Then the sample simulation is performed with an additive noise of 5 db and -5 db. The corresponding normalized outputs are given in Fig 3.10 (c) and Fig 3.10(d) respectively.

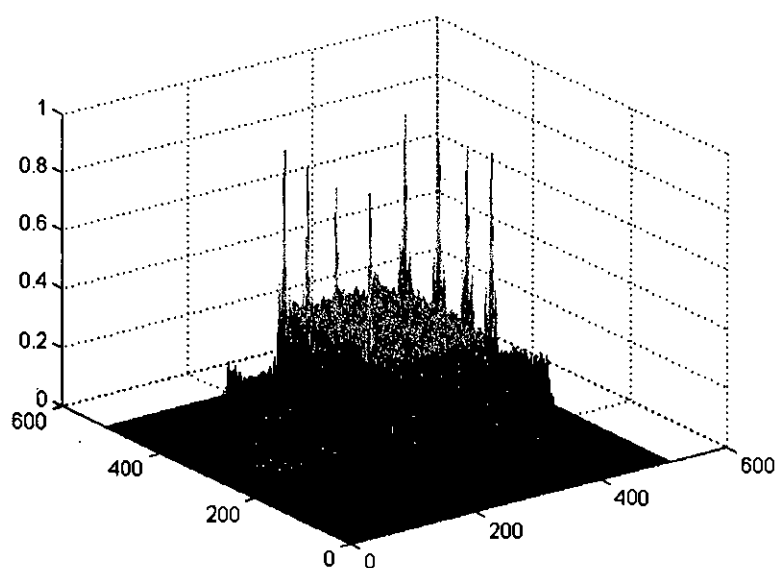


Fig. 3.10 (c) Normalized correlation output SNR of 5db.

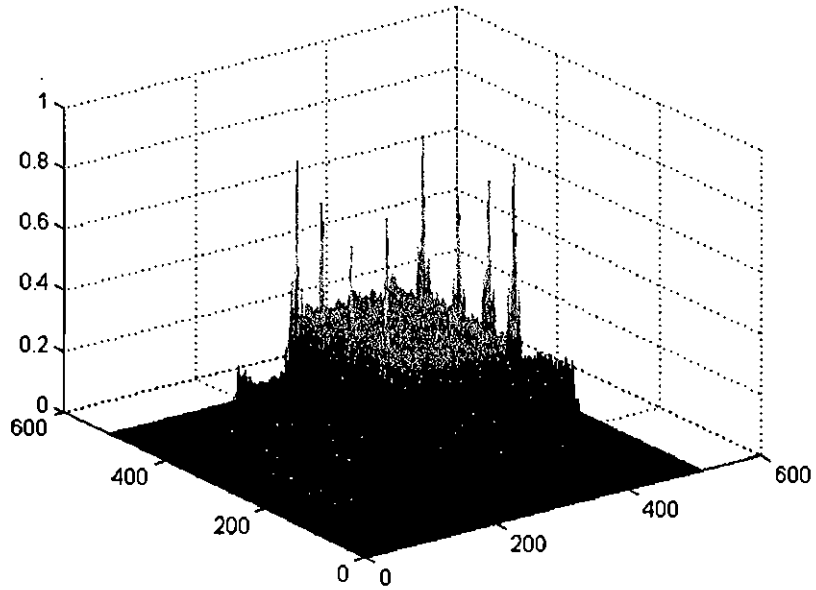


Fig. 3.10 (d) Normalized correlation output SNR of -5db.

If we apply the post processing technique to the outputs obtained in the Fig 3.10(b), Fig 3.10(c) and Fig 3.10(d) we get the post processed normalized correlation output as given in Fig 3.10(e), Fig 3.10(f) and Fig 3.10(g) respectively.

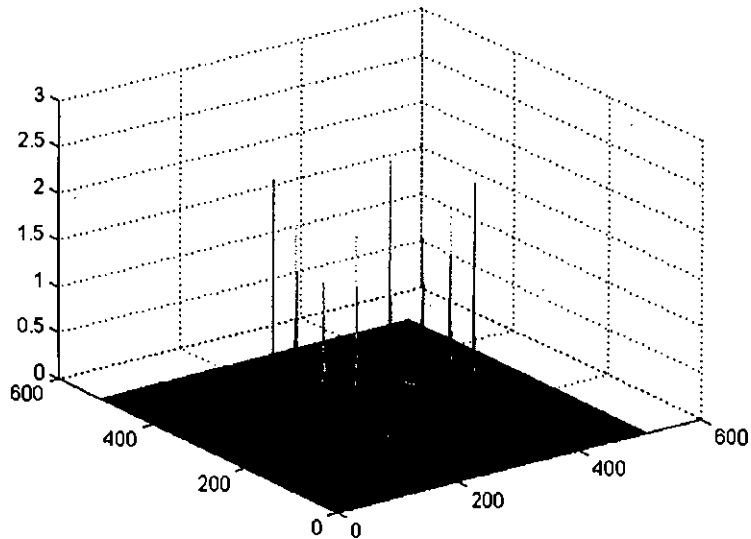


Fig. 3.10 (e) Post processed normalized correlation output SNR of 0db.

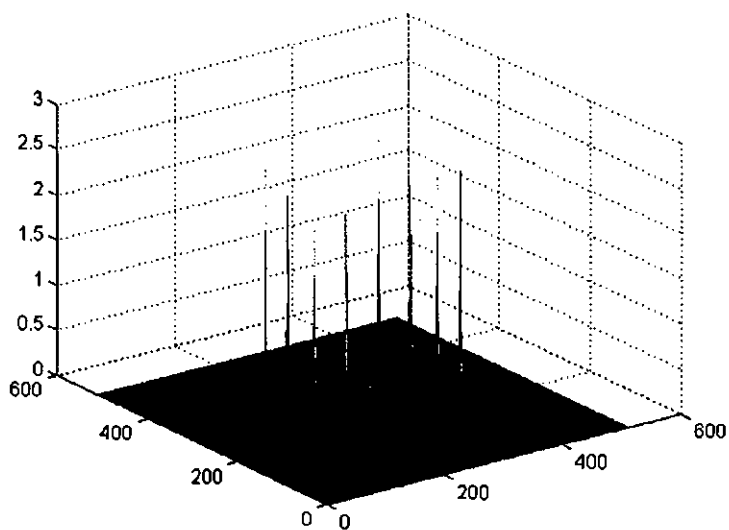


Fig. 3.10 (f) Post processed normalized correlation output SNR of 5db.

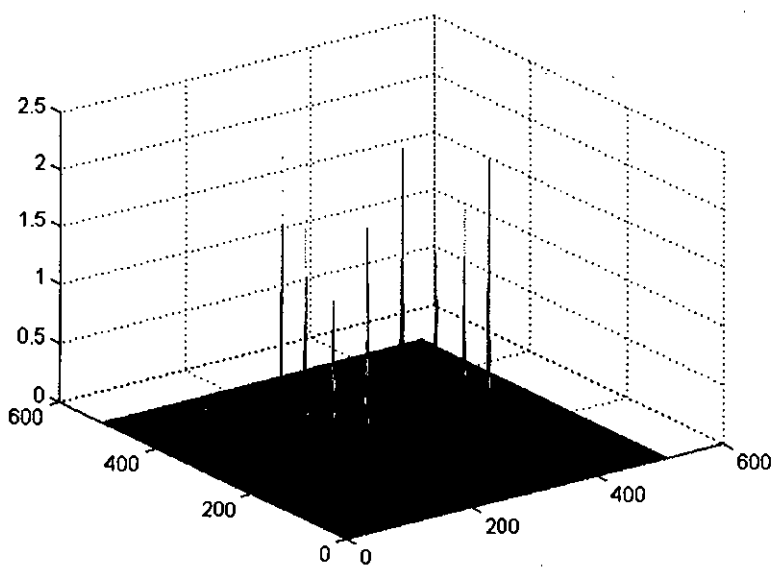


Fig. 3.10 (g) Post processed normalized correlation output SNR of -5db.

100884

3.7.1.2 Performance Evaluation

The summary of detection performance of the normalized correlation technique in noisy conditions are given without post processing in Table 3.6 and with post processing in Table 3.7.

Table 3.8: Detection performance binary images containing targets only in noisy conditions without post processing.

Performance Criteria	SNR 5db	SNR 0db	SNR -5db
Normalized CPI	0.9933, 0.9861, 0.9766, 0.9512	0.9803, 0.9606, 0.9367, 0.8794	0.9461, 0.8990, 0.8496, 0.7509
FWHM	4	6	9
PSR	1.905	1.802	1.726

Table 3.9: Detection performance binary images containing targets only in noisy conditions with post processing.

Performance Criteria	SNR 5db	SNR 0db	SNR -5db
Normalized CPI	1.00, 0.9716, 0.9354, 0.845	1.00, 0.924, 0.84, 0.71	1.00, 0.827, 0.778, 0.623
FWHM	1	2	2
PSR	6.93	6.29	5.4

From the tables, the target peaks (CPI) are successively lowered with the addition of more and more noise in the input scene. It is observed that with such noise the correlation output is good enough to detect the targets. Post processing technique also decreases the FWHM, which provides sharper peaks. The PSR is also high in the case of post-processed output in all of the noisy input scenes. So by using suitable threshold value, the target peaks can be easily extracted in the midst of spurious signal generated due to noisy signal.

3.7.1.3 Binary Image Containing Targets and Non-Targets

To investigate if the system works well for the binary image containing targets and non-targets, joint image of Fig 3.11(a) is taken with an additive white noise of 0db in the input scene. Fig 3.11(b) and Fig 3.11(c) shows the corresponding correlation output without and with post processing.

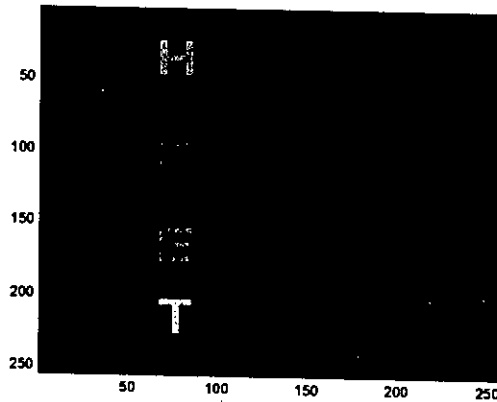


Fig. 3.11 (a) Joint image with an additive white noise of 0db

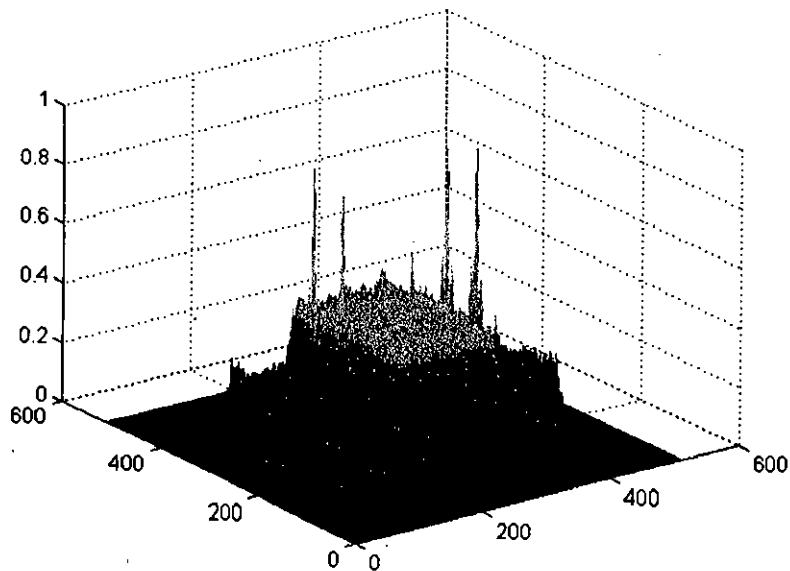


Fig. 3.11 (b) Correlation output an additive white noise of 0db without post processing

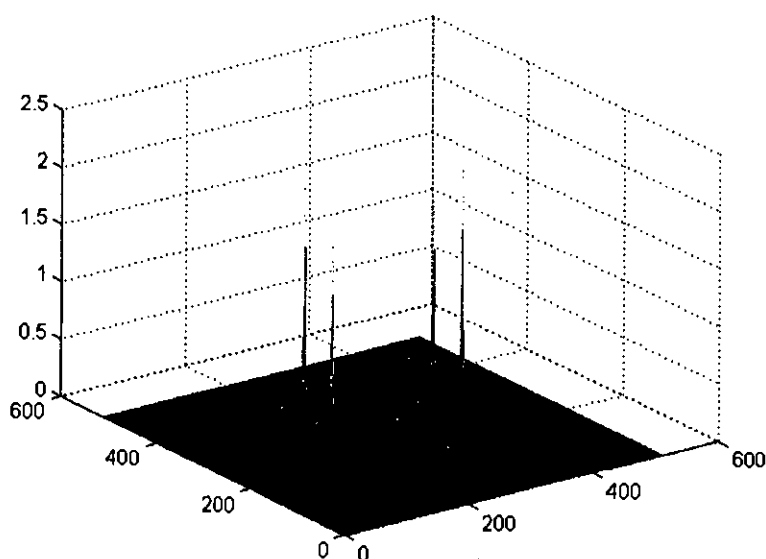


Fig. 3.11 (c) Correlation output an additive white noise of 0db with post processing

3.7.1.4 Performance Evaluation

The summary of detection performance of the normalized correlation technique in noisy conditions with input scene containing targets and non-targets are given without post processing in Table 3.8 and with post processing in Table 3.9.

Table 3.10: Detection performance binary images containing targets and non targets in noisy conditions without post processing.

Performance Criteria	SNR 5db	SNR 0db	SNR -5db
Normalized CPI	0.9819, 0.9617, 0.5503, 0.5484	0.9500, 0.9022, 0.5587, 0.5548	0.8767, 0.7877, 0.5467, 0.5409
PCR	1.74	1.61	1.44
FWHM	4	6	18
PSR	1.80	1.70	1.60

Table 3.11: Detection performance binary images containing targets and non targets in noisy conditions with post processing.

Performance Criteria	SNR 5db	SNR 0db	SNR -5db
Normalized CPI	1.00, 0.922, 0.162, 0.160	1.00, 0.825, 0.191, 0.188	1.00, 0.72, 0.24, 0.23
PCR	5.68	4.30	2.88
FWHM	1	2	2
PSR	6.16	5.02	4.11

From the tables, discrimination ratios between target peak and non-target peak (PCR) are successively lowered with the addition of more and more noise in the input scene. With the noise of 0db the ratio becomes 1.61. Since in comparative judgment, here the target peak is at least 1.61 times higher than the non-target peak and this is appreciable limit for threshold. The post processing increases this PCR to 4.30, which increases the detection efficiency as well. Therefore by using suitable threshold value, the target peaks can be easily extracted in the midst of non-targets peaks and other spurious signal generated due to noisy signal.

3.7.2 Noisy Gray Level Image detection

3.7.2.1 Simulation Results

To investigate the noise robustness of the system to gray level images, additive gaussian white noise is added in the input scene. Fig 3.12(a) shows the joint image with an additive white noise of 0db in the input scene of lena. Fig 3.12(b) shows the corresponding normalized correlation output of Fig 3.12(a). Post-processed normalized correlation output is also shown in Fig 3.12(c).

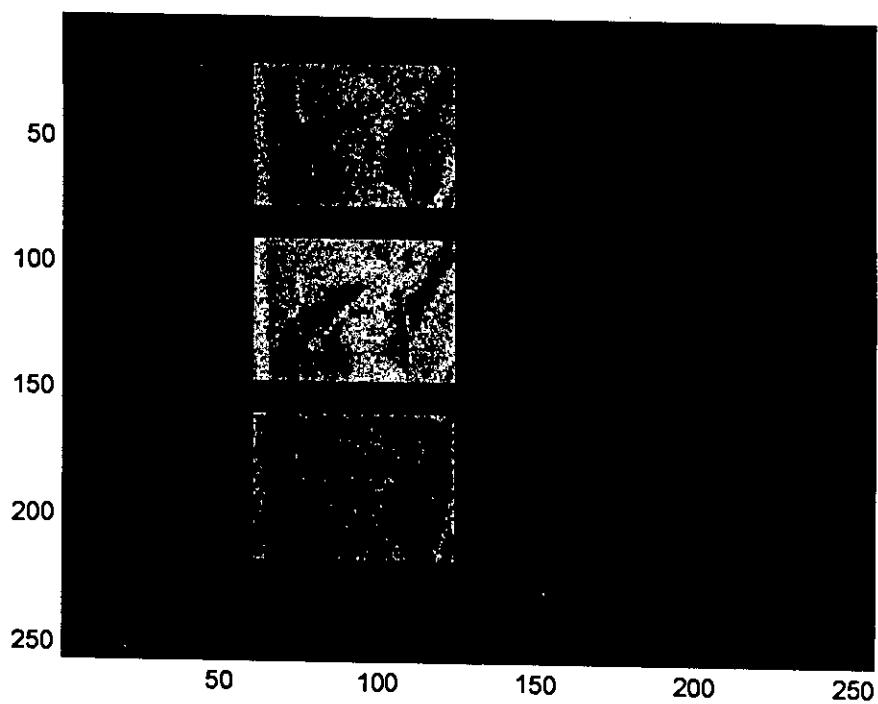


Fig. 3.12 (a) Input scene image with an additive white noise of 0db

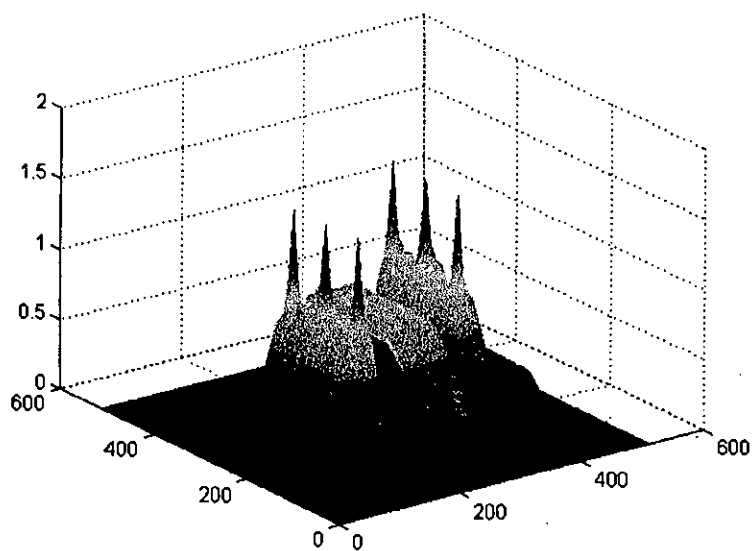


Fig. 3.12 (b) Normalized correlation output without post processing for SNR=0db

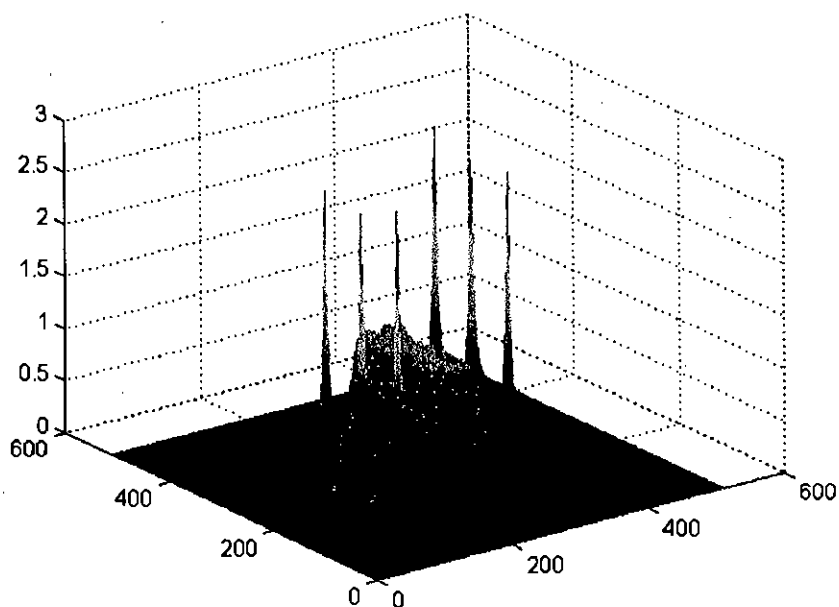


Fig. 3.12 (c) Normalized correlation output with post processing for SNR=0db

3.7.2.2 Performance Evaluation

The summary of detection performance of the normalized correlation technique in noisy conditions with input scene containing targets and non-targets are given without post processing in Table 3.10 and with post processing in Table 3.11.

Table 3.12: Detection performance of gray level in noisy conditions without post processing.

Performance Criteria	SNR 5db	SNR 0db	SNR -5db
Normalized CPI	1.00, 1.00, 0.99	1.00, 0.988, 0.967	1.00, 0.967, 0.944
FWHM	438	830	1578
PSR	1.30	1.23	1.15

Table 3.13: Detection performance of binary images in noisy conditions with post processing.

Performance Criteria	SNR 5db	SNR 0db	SNR -5db
Normalized CPI	1.00, 1.00, 0.95	1.00, 1.00, 0.967	1.00, 0.955, 0.930
FWHM	32	289	1254
PSR	2.26	2.12	1.95

From the tables, it can be observed that the proposed scheme is valid for gray level images in noisy conditions as well. The FWHM increases with the addition of more and more noise. But the post processing lowers this value significantly. Again the PSR is high enough to detect the targets. So by using suitable threshold value, the target peaks can be easily extracted in the midst of spurious signal generated due to noisy signal although the input is a gray level image.

3.7.2.3 Comparative Analysis

For a comparative study of the normalized joint transform correlator with the morphological correlation based joint transform correlator, we analyzed the time required for detection of binary and gray scale images with the input scene noise of 0dB. Both techniques were run using the MATLAB 5.3 and a 2.4 GHz Pentium processor. The following table gives the results.

Table 3.14: Comparative analysis of normalized JTC with the morphological JTC

Detection Method	Binary Image 0dB SNR Detection time (sec)	Gray Level Image 0dB SNR Detection time (sec)
Normalized JTC without post processing	3.3440	3.6809
Normalized JTC with post processing	3.4680	3.9528
Morphological based JTC	7.0156	7.7580

Here we can see that if there is noise in the input scene, the NJTC is faster than the morphological based correlator when detecting noisy binary and gray level images.

3.8 Modified Normalized Correlation

3.8.1 Theoretical Analysis

We can introduce a modification in the normalized correlation technique described and reduce a processing step and decrease the detection time significantly.

The normalized correlation is given by,

$$N(x', y') = \frac{1}{c} \frac{[t(x', y') \otimes r(x', y')]^2}{t^2(x', y') \otimes s(x', y')} \quad (3.19)$$

If we replace the denominator $t^2(x', y') \otimes s(x', y')$ with $[t(x', y') \otimes s(x', y')]^2$ the normalized correlation becomes,

$$\begin{aligned} N(x', y') &= \frac{1}{c} \frac{[t(x', y') \otimes r(x', y')]^2}{[t(x', y') \otimes s(x', y')]^2} \\ &= \frac{1}{c} \left[\frac{t(x', y') \otimes r(x', y')}{t(x', y') \otimes s(x', y')} \right]^2 \end{aligned} \quad (3.20)$$

Although $[t^2(x', y') \otimes s(x', y')] \neq [t(x', y') \otimes s(x', y')]^2$, they have almost the same effect of normalizing the target.

If we do the above modification, it is not necessary to compute the square of the target in the second input plane, so we do not have to wait for the square of the target to be computed rather we would put the target image in the second input plane directly. This would reduce the processing time significantly and the need for high dynamic range SLM is minimized.

So here two input planes each consisting of two inputs will be employed. The first input plane displays the reference image $r(x, y)$ and target image $t(x, y)$ while the second input

plane shows the square of the target image $t(x,y)$ and support of the reference $s(x,y)$. Both of the input planes are illustrated in the Fig 3.13(a). The first input plane can be considered as the combination of two joint images described as

$$f_1(x, y) = t(x + a, y - b) + r(x - a, y + b) \quad (3.21)$$

And the second input planes can be considered as the combination of two joint images in expressed as

$$f_2(x, y) = t(x + a, y - b) + s(x - a, y + b) \quad (3.22)$$

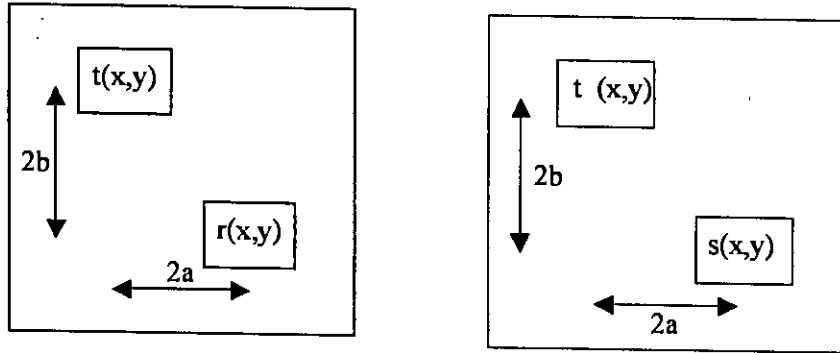


Fig. 3.13(a) First and second input planes with the joint images

Now the corresponding correlation output in the first output plane will be as

$$f_1'(x, y) = r(x, y) \otimes t(x, y) * \delta(x + 2a, y - 2b) + t(x, y) \otimes r(x, y) * \delta(x - 2a, y + 2b) \quad (3.23)$$

Similarly the corresponding correlation output in the second output plane will be as

$$f_2'(x, y) = s(x, y) \otimes t^2(x, y) * \delta(x + 2a, y - 2b) + t^2(x, y) \otimes s(x, y) * \delta(x - 2a, y + 2b) \quad (3.24)$$

The output plane correlation distribution of both the input planes are shown in Fig. 3.13(b) as follows

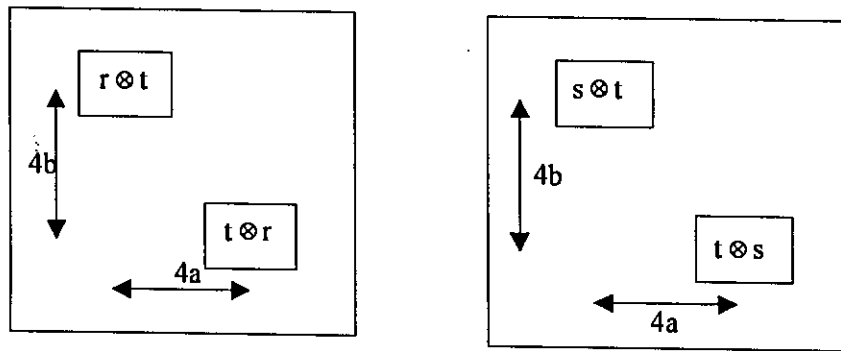


Fig. 3.13(b) Output planes with correlation distribution

Pixel wise division of the first output plane with the second output plane and squaring the result using a computer will yield to give the modified normalized correlation. Extraction of the desired terms is easy as they are the only ones left after the Fourier plane image subtraction technique is employed. So false peaks are eliminated and fewer correlation terms are produced at the output planes, which results an increase in detection efficiency.

3.8.2 Simulation Results

3.8.2.1 Binary Image Detection

To analyze the performance of the above-modified scheme, a binary character 'E' of English Alphabet has been taken as the reference image. The size of the character is 32×32 pixels and it is placed in a joint image of size 256×256 pixels. The joint image contains multiple objects (target and non-targets) as shown in Fig. 3.14(a). Two non targets, 'H' and 'T', of four and seven times illumination intensity, respectively, and two targets, 'E' of similar and two times illumination intensity than the reference image, 'E' have been considered. The simulations are performed using FFT2 routine of MATLAB software and the outputs are plotted using the 3-D plotting routine.

The correlation output in Fig 3.14(b) shows four cross-correlation peaks for the targets and non-targets. Two peaks are of same height and represent the targets. Although the intensity of 'H' and 'T' are stronger than the targets, the cross correlation peaks are found to be much lower than the auto correlation peaks produced by the targets. So the modified normalized recognition leads to proper detection of targets under different illumination. Table 3.12 gives the summary of detection performance of the modified technique of targets and non-targets under varying illumination.

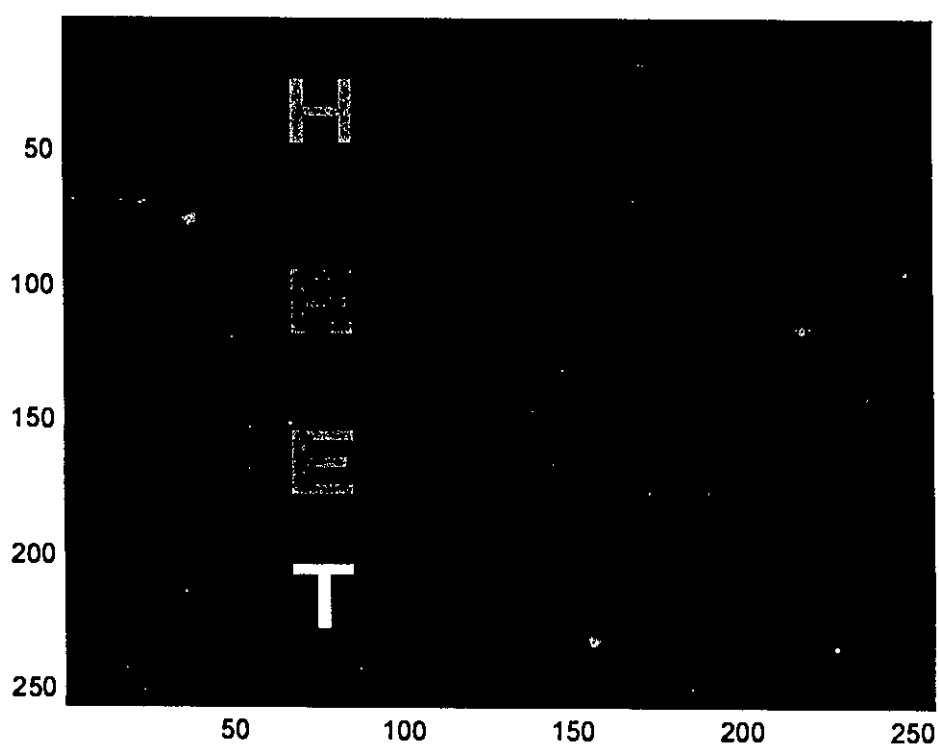


Fig. 3.14(a) Input joint image with multiple targets and non-targets

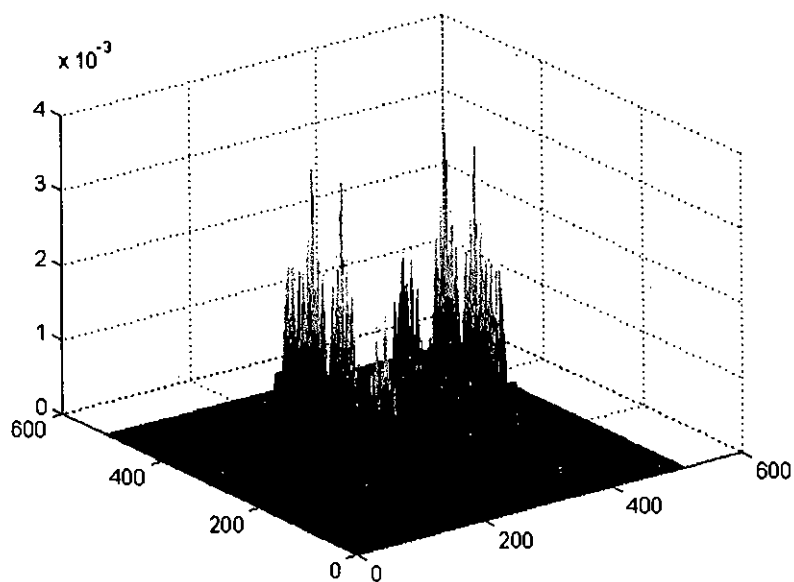


Fig. 3.14(b) Modified normalized correlation output of input joint image with multiple targets and non-targets before post processing.

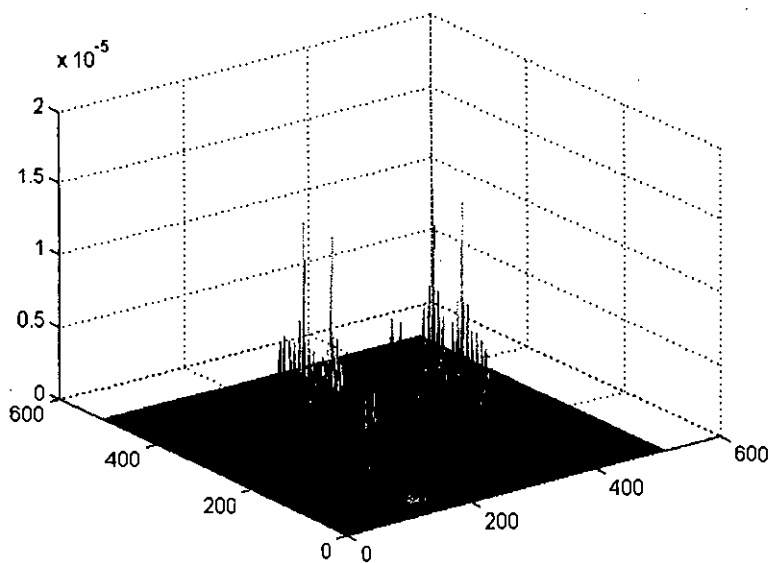


Fig. 3.14(c) Modified normalized correlation output of input joint image with multiple targets and non-targets after post processing.

Table 3.15: Detection performance of binary images consisting of targets and non-targets with post processing.

Performance Criteria	Normalized JTC with Post processing	Modified Normalized JTC with post processing
Normalized CPI	1.00, 1.00	1.00, 1.00
PCR	7.612	1.8
FWHM	1.00	5
PSR	7.94	1.82

From the Table 3.12 we can see that the modified normalized technique produces peak heights of equal strength and lead to proper target detection. Performance in respect to PCR, FWHM and PSR degraded a little bit, but still in comparative judgment with the non-target peaks, there is still an appreciable limit for threshold. Therefore, by using suitable threshold value, the targets peaks can be easily extracted by using the modified normalized correlation technique.

Validity of the modified technique also holds good for input scene containing only targets with varying illumination. If four targets "E" are taken in the input scene and of varying illumination then the correlation output without and with post processing is given in the Fig 3.15(a) and Fig 3.15(b). Detection performance of the current configuration is given in the Table 3.13. The modified technique gives the same CPI and the PSR and FWHM are within ranges of detecting the targets successfully.

Table 3.16: Detection performance of binary images consisting of targets only with post processing.

Performance Criteria	Normalized JTC with Post processing	Modified Normalized JTC With post processing
Normalized CPI	1.00, 1.00, 1.00, 1.00	1.00, 1.00, 1.00, 1.00
FWHM	1.00	5
PSR	7.94	1.79

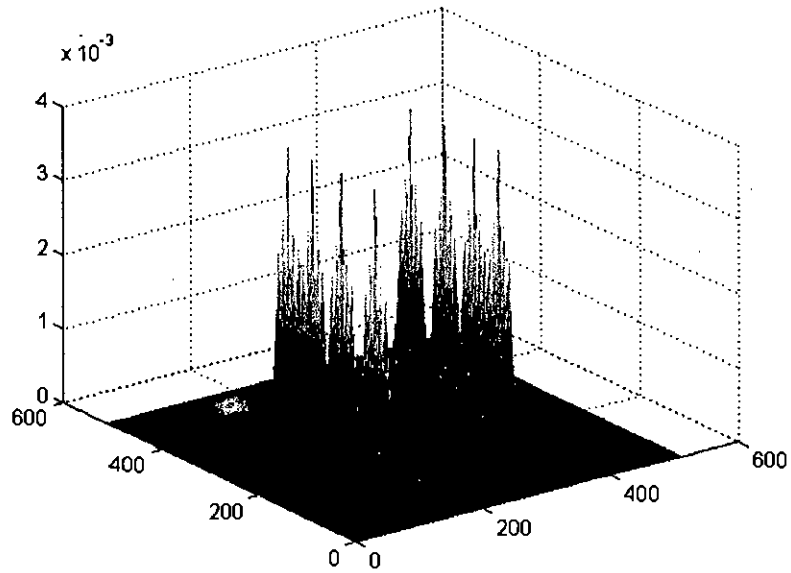


Fig. 3.15(a) Modified normalized correlation output of input joint image with multiple targets only before post processing.

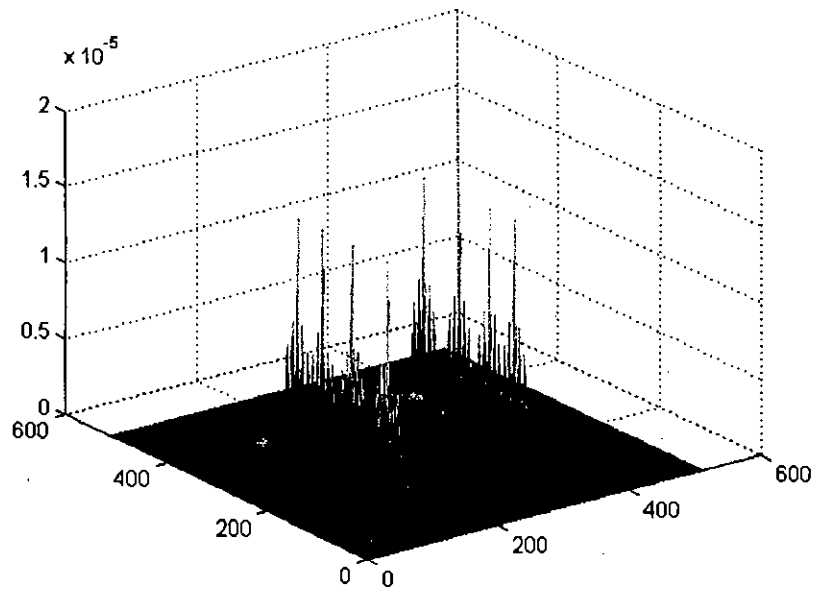


Fig. 3.15(b) Modified normalized correlation output of input joint image with multiple targets only after post processing.

3.8.2.2 Gray Level Image Detection

To investigate if the modified normalized correlation technique works well on the gray level images, we take the image 'lena' and the same target distribution as described before. The correlation output without post processing is given in Fig 3.16(a). Table 3.14 summarizes the detection performance comparing the modified technique with the normalized correlation technique.

Table 3.17: Detection performance of gray level images using the modified normalized correlation technique.

Performance Criteria	Normalized JTC without Post processing	Modified Normalized JTC without post processing
Normalized CPI	1.00, 0.9841, 0.9583	1.00, 0.753, 0.727
FWHM	471	184
PSR	1.29	1.25

From Table 3.14, although the target peaks in the modified technique reduces but we can accept it for pattern recognition purpose and there is no deterioration of the visibility of the targets. The PSR is found to be almost equal in value.

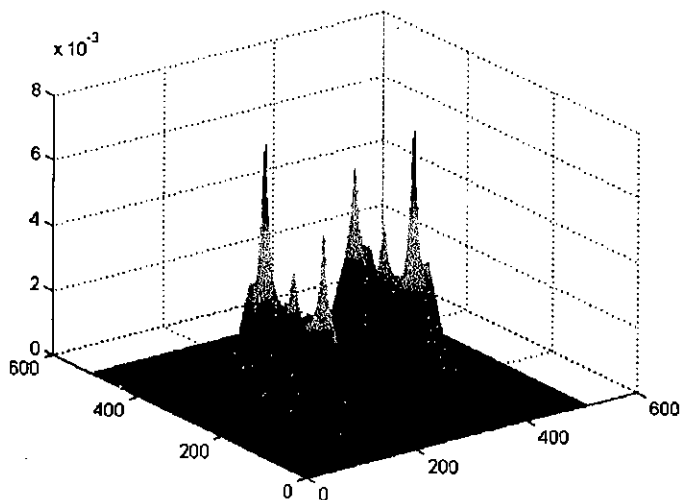


Fig. 3.16(a) Modified correlation output of gray level images without post processing.

3.8.2.3 Noisy Image Detection

Let us investigate the outcome of the modified normalized correlation technique when we apply a random noise with signal to noise ratio (SNR) of 0dB. Fig 3.17(a) and Fig 3.17(b) gives the output when the target contains only targets and when there are targets and non-targets in the input scene respectively. In both cases we see that the output is good enough for pattern recognition purposes as there is no deterioration of the visibility of target peaks due to the introduction of noise. Again Fig 3.17(c) gives the modified correlation output for gray level images. Although there is a lot of side lobes and other peaks, still from the output we can conclude on the number of targets properly. So the modified system is feasible for target detection purposes even in the midst of noise.

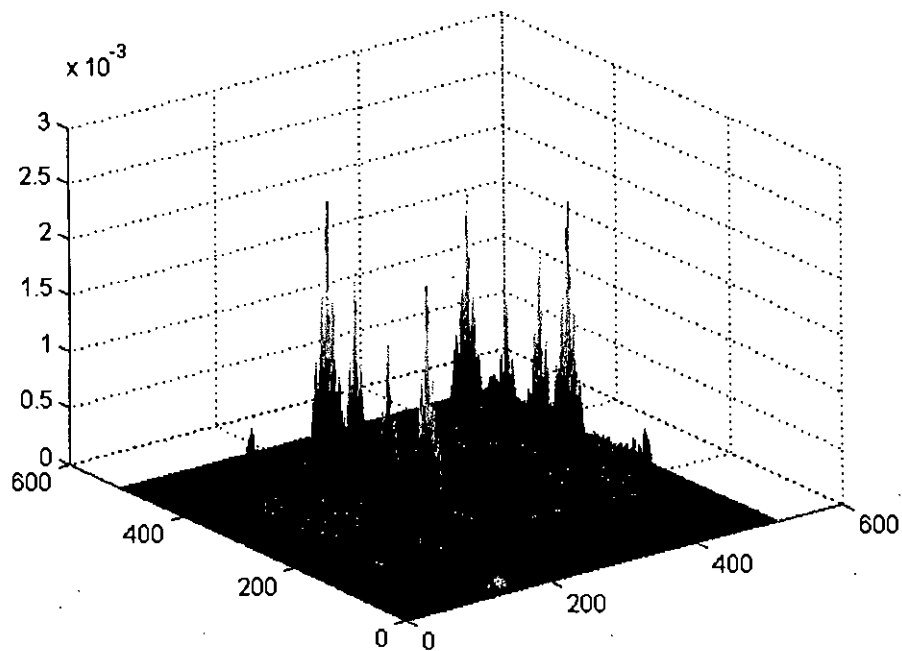


Fig. 3.17(a) Modified correlation output of noisy input scene with only targets.

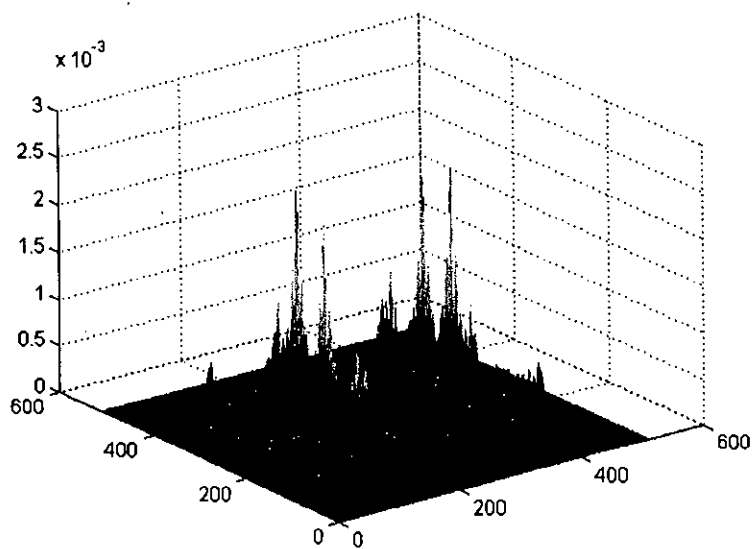


Fig. 3.17(b) Modified correlation output of noisy input scene with targets and non-targets present.

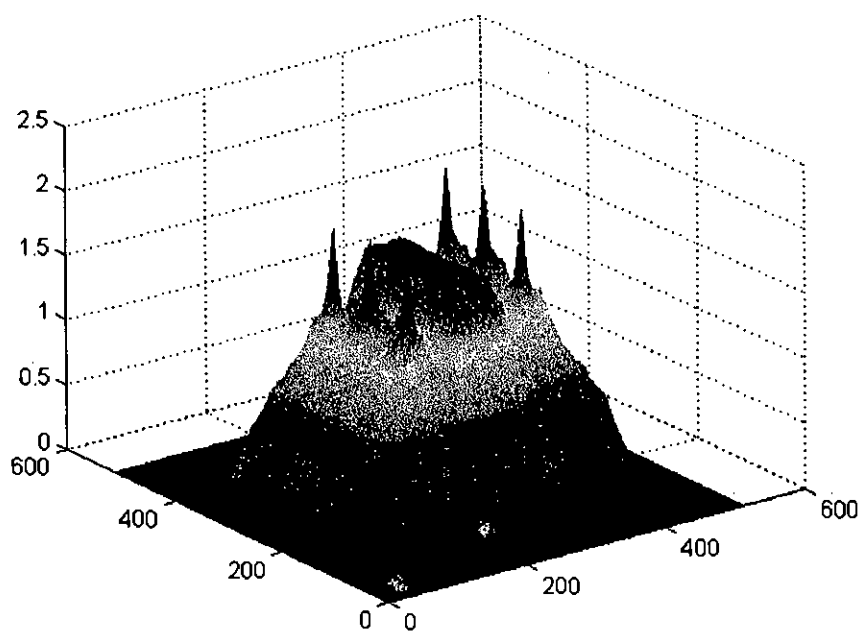


Fig. 3.17(c) Modified correlation output of noisy input scene with gray level images.

3.8.2.4 Comparative Analysis

For a comparative study of the modified normalized joint transform correlator with the morphological correlation based joint transform correlator, we analyzed the time required for detection of binary and gray scale images without and with the input scene noise of 0dB. Both techniques were run using the MATLAB 5.3 and a 2.4 GHz Pentium processor. The following table gives the results.

Table 3.18: Comparative analysis of normalized JTC with the morphological JTC

Detection Method	Binary Image	Gray Level Image	Binary Image	Gray Level Image
	Detection time (sec)	Detection time (sec)	0dB SNR Detection time (sec)	0dB SNR Detection time (sec)
Normalized JTC with post processing	3.2820	3.7350	3.4680	3.9528
Modified Normalized JTC with post processing	3.0188	3.5021	3.2540	3.7785
Morphological based JTC	6.7370	7.0256	7.0156	7.7580

From the table, we can see that the modified normalized JTC decrease the detection time about 0.2 sec and it is faster in respect to binary or gray scale images without or with noise in the input scene.

3.9 Conclusion

In this chapter a novel technique for intensity invariant pattern recognition is proposed which employs normalized joint transform correlation. The proposed technique is done in the space domain by utilizing the real-time correlation capability of JTC. This technique overcomes the limitation of currently available normalized correlation filters that are realized in the frequency domain and not suitable for real-time pattern recognition because of the requirements of filter fabrication. Again this algorithm

produces only four desired correlation terms in the output plane which increases the detection efficiency as well. Compared to the morphological correlator which can also achieve the same effect as the normalization in some situations, the proposed scheme has better processing speed as it utilizes linear correlation than that of morphological correlation which is slower in computation. This technique can detect targets from an input scene at any condition of non-target and also in the presence of noise. Computer simulation confirms the effectiveness of the technique in multiple target detection. Where some of the previous method fails, the proposed algorithm is valid for intensity varying gray scale images as well. Simulation results prove the validity of the proposed method.

Chapter 4

CONCLUSIONS

4.1 Conclusion

Joint transform correlators are widely used for pattern recognition or pattern classification. They provide real time detection of the targets with very high optical efficiency and reduced cost. Since the advent of joint transform correlators, various works have been performed on it and various modifications or improvements have been proposed. Among the various forms of joint transform correlation techniques, the fringe-adjusted joint transform correlation and recently devised multi-target detection algorithm are suitable for successful detection of objects or images when there are multiple targets and non-targets in the input scene. Both of these techniques produce a pair of peaks for each target object. But if the intensity of the target images is higher than the reference image then the intensity of the false alarm may be higher than the desired cross-correlation peaks and therefore simply obscures the detection. So recognition of targets under transformation of intensity should be introduced.

In this work, a method for getting intensity invariance optical pattern recognition in real time has been developed. The Cauchy-Schwarz inequality has been applied to correlation filters in order to get normalization to achieve intensity invariance. In the proposed method, an efficient implementation of normalized correlation in the space domain has been proposed to achieve real time discrimination between intensity varying similar non-targets. The proposed method also performs well even in the midst of noise in the input scene.

Two input planes each consisting of two inputs has been employed. The first input plane displays the reference image and target image while the second input plane shows the square of the target image and support of the reference. After performing Fourier transformation to both of the channels, image subtraction technique has been used to the

joint power spectrum (JPS) to eliminate false peaks and to produce only the desired peaks. The magnitude of the resultant JPS is then inverse Fourier transformed and we obtain output plane correlation distribution for both of the input planes. By squaring the first output plane and performing a pixel wise division operation with the second output plane, we get the intensity invariant correlation peaks. To achieve higher discrimination ratio between similar non-target objects a post processing technique has been also introduced.

We can introduce a modification in the normalized correlation technique described and reduce a processing step to decrease the detection time significantly. If we do the above modification, it is not necessary to compute the square of the target in the second input plane, so we do not have to wait for the square of the target to be computed rather we would put the target image in the second input plane directly. This would reduce the processing time significantly and the need for high dynamic range SLM is minimized. Computer simulation validates the proposed modification to the above technique.

In this thesis work, the binary images of English block-lettered alphabets are used to show and testify the performance of the proposed schemes for intensity varying targets. Again to show that the method is successful in determining targets, intensity varying gray level image 'lena' was used. The effectiveness in discrimination between gray level targets and non-targets has been analyzed by taking two different closely similar gray-level car images. The developed optical correlator gives almost equal correlation peaks for all the targets, whether the targets are brighter or darker than the reference and whether there is noise in the input scene or not. Therefore, it can be said that the proposed scheme is a successful one though more works can be done on it for further excellence.

4.2 Future Works

In this work, emphasis is given on the recognition of images, which are of varying illumination. There may be distortion introduced by in-plane or out-of-plane rotation of still object. So a projection-slice synthetic discriminant function (SDF) may be used for such case. According to the projection-slice theorem a 1-D Fourier transform along a projected line in an image corresponds to a slice in the 2-D Fourier transform of that image along the same line. By taking different slices from the training images, a composite image can be created such that it is tolerant to intensity fluctuations and in-plane or out-plane rotation.

Again, in this work, the target detection operation is performed on a stationary image. Here the object is assumed to be still. In case of moving objects, another important application arises that is target tracking from moving objects. In this case frame-based analysis is important. A set images or frames are taken and the object is identified from each of this frame. Finally, a trajectory of the moving object can be plotted to trace the future position of the object.

On the other hand, all real objects are color objects and contain more information than binary or gray level images. To properly represent an object it must be represented in color image. Hence this work can also be extended by analyzing or experimenting with color image. Therefore, to deal with color images, three basic colors i.e. 'red', 'green' and 'blue' have to be extracted from the actual image and would have to be processed using three channels. Then three channels can be adopted independently for these three colors. At the end the output from these three channels may be fused to get the final or actual correlation output.

All of these are an overview of future works in this field. Further study and detailed analysis is required in every case to implement the purpose.

REFERENCES

- [1] Robert Schalkoff, "Pattern Recognition, Statistical Structural and Neural Approaches," John Wiley & Sons, New York, 1992.
- [2] Richard O. Duada, Peter E. Hart, David G. Stork, "Pattern Classification," Second Edition, Wiley-Interscience, 2000.
- [3] B. Yegnarayana, "Artificial Neural Networks," Prentice-Hall, India, 2003.
- [4] Rafael C. Gonzalez, Richard E. Woods, "Digital Image Processing," Addison-Wesley Publishing Company, Inc., 1992.
- [5] S. M. Attaullah Bhuiyan, "Distortion invariant class-associative target detection using joint transform correlation," M. Sc. Thesis, Department of EEE, BUET, 2003.
- [6] J. W. Goodman, "Introduction to Fourier Optics," McGraw Hill, New York, 1968.
- [7] Eugene Hecht and Alfred Zajac, "Optics," Addison-Wesley Publishing Company, Philippines, 1979.
- [8] A. VanderLugt, "Signal detection by complex spatial filtering," *IEEE Trans. Inf. Theory* IT-10, pp. 139-146, 1964.
- [9] H. J. Caulfield and R. Haimes, "Generalized matched filtering," *Appl. Opt.*, Vol. 18, No. 2, pp. 181-183, 1980.
- [10] D. A. Gregory, "Real-time pattern recognition using a modified LCTV in a coherent optical correlator," *Appl. Opt.*, Vol. 25, pp. 467-469, 1986.
- [11] A. D. Gara, "Real-time tracking of moving objects by optical correlation," *Appl. Opt.*, Vol. 18, pp. 172-172, 1989.
- [12] A. Mahalanobis and D. Casasent, "Performance evaluation of minimum average correlation filters," *Appl. Opt.*, Vol. 30, pp. 561-571, 1991.
- [13] R. R. Kallman and D. H. Goldstein, "Phase-encoding input image for optical pattern recognition," *Opt. Eng.*, Vol. 33, pp. 1806-1813, 1994.
- [14] D. Casasent and A. Furman, "Sources of correlation degradation," *Appl. Opt.*, Vol. 16, pp. 1652-1661, 1977.
- [15] X. J. Lu, F. T. S. Yu and D. A. Gregory, "Comparison of VanderLugt and joint transform correlator," *Appl. Phys. B. Photophys. Laser Chem.*, Vol. 51, pp. 153-164, 1990.
- [16] Purwardi Purwosumarto and Francis T. S. Yu, "Robustness of joint transform correlator versus VanderLugt correlator," *Opt. Eng.*, Vol. 36, No. 10, pp. 2775-2780, 1997.
- [17] C. S. Weaver and J. W. Goodman, "A technique for optically convolving two functions," *Opt. Commun.*, Vol. 52, No. 7, pp. 1248-1249, 1966.
- [18] F. T. S. Yu and X. J. Lu, "A real-time programmable joint transform correlator," *Opt. Commun.*, Vol. 52, No. 10, pp. 10-16, 1984.
- [19] F. T. S. Yu, S. Jutamulia, T. W. Lin and D. A. Gregory, "Adaptive real-time pattern recognition using a liquid crystal TV based joint transform correlator," *Appl. Opt.*, Vol. 26, pp. 1370-1372, 1988.

- [20] B. Javidi and C. Kuo, "Joint transform image correlation using a binary spatial light modulator at the Fourier plane," *Appl. Opt.*, Vol. 27, pp. 663-665, 1988.
- [21] S. K. Rogers, J. D. Cline and M. Kabrisky, "New binarization techniques for joint transform correlation," *Opt. Eng.*, Vol. 29, No. 9, pp. 1018-1023, 1990.
- [22] B. Javidi, J. Wang and Q. Tang, "Multiple-object binary joint transform correlation using multiple-level threshold crossing," *Appl. Opt.*, Vol. 31, No. 29, pp. 4816-4822, 1992.
- [23] M. S. Alam and M. A. Karim, "Improved correlation discrimination in a multiobject bipolar joint transform correlator," *Opt. & Laser Tech*, Vol. 24, pp. 45-50, 1992.
- [24] W. B. Hahn and D. L. Flannery, "Design elements of a binary joint transform correlator and selected optimization techniques," *Opt. Eng.*, Vol. 31, No. 5, pp. 896-905, 1992.
- [25] F. T. S. Yu, F. Cheng, T. Nagata and D. A. Gregory, "Effects of fringe binarization of multi-object joint transform correlation," *Opt. Eng.*, Vol. 28, No. 5, pp. 2988-2990, 1989.
- [26] Q. Tang and B. Javidi, "Multiple-object detection with a chirp-encoded joint transform correlator," *Appl. Opt.*, Vol. 32, pp. 4344-4350, 1993.
- [27] S. Jutamulia, G. M. Storti, D. A. Gregory and J. C. Kirsch, "Illumination-independent high-efficiency joint transform correlation," *Appl. Opt.*, Vol. 30, No. 29, pp. 4173-4175, 1991.
- [28] C. Li, S. Yin and F. T. S. Yu, "Nonzero-order joint transform correlator," *Opt. Eng.*, Vol. 37, No. 1, pp. 58-65, 1998.
- [29] M. S. Alam and Y. A. Gu, "Improving multi-object correlation discrimination using data fusion in the correlation plane," *Optik*, Vol. 106, No. 1, pp. 1-6, 1997.
- [30] G. Lu, Z. Zhang, S. Wu and F. T. S. Yu, "Implementation of a non-zero order joint transform correlator by use of phase shifting techniques," *Appl. Opt.*, Vol. 36, No. 2, pp. 470-483, 1997.
- [31] S. Jutamulia and D. A. Gregory, "Soft blocking of the dc term in Fourier optical systems," *Opt. Eng.*, Vol. 37, No. 1, pp. 49-51, 1998.
- [32] F. T. S. Yu, C. Li and S. Yin, "Comparison of detection efficiency of nonzero-order and conventional joint transform correlation," *Opt. Eng.*, Vol. 37, No. 1, pp. 52-57, 1998.
- [33] M. S. Alam and M. A. Karim, "Fringe-adjusted joint transform correlator," *Appl. Opt.*, Vol. 32, No. 23, pp. 4344-4350, 1993.
- [34] M. S. Alam and M. A. Karim, "Joint transform correlation under varying illumination," *Appl. Opt.*, Vol. 32, pp. 4344-4350, 1993.
- [35] M. S. Alam, "Fractional power fringe-adjusted joint transform correlator," *Opt. Eng.* Vol. 34, pp. 3208-3216, 1995.
- [36] M. S. Alam, "Phase-encoded fringe-adjusted joint transform correlation," *Opt. Eng.*, Vol. 39, No. 5, pp. 1169-1176, 2000.

- [37] J. Khoury, G. Asimellis and C. Woods, "Incoherent-erasure nonlinear joint transform correlator," *Opt. Lett.*, Vol. 20, pp. 2321-2323, 1995.
- [38] M. S. Alam and J. Khoury, "Fringe-adjusted incoherent-erasure joint transform correlator," *Journal of Optical Engineering*, Vol. 37, pp. 75-82, 1998.
- [39] M. S. Alam and M. A. Karim, "Multiple target detection using a modified fringe-adjusted joint transform correlator," *Opt. Eng.*, Vol. 33, pp. 1610-1617, 1994.
- [40] M. S. Alam, "Multi-target photo refractive fringe-adjusted joint transform correlation," *Journal of Optical memory and Neural Networks*, Vol. 6, pp. 287-296, 1998.
- [41] A. A. S. Awwal, M. A. Karim and S. R. Jahan, "Improved correlation discrimination using an amplitude modulated phase-only filter," *Appl. Opt.*, Vol. 29, pp. 233-236, 1990.
- [42] T. Nomura, "Phase-encoded joint transform correlator to reduce the influence of extraneous signals," *Appl. Opt.*, Vol. 37, pp. 3651, 1998.
- [43] G. Lu and F. T. S. Yu, "Performance of a phase transformed input joint transform correlator," *Appl. Opt.*, Vol. 35, pp. 304, 1996.
- [44] M.S. Alam and M.A. Karim, "Joint transform correlation under varying illumination," *Appl Opt*, Vol 32, pp.4351-4356, 1993.
- [45] R. Kotynski and K.C. Macukow, "Optical pattern recognition based on normalized correlation," *SPIE Proceedings*, Vol. 3904, pp.228-239, 1999.
- [46] F. M. Dickey and L.A. Romero, "Normalized correlation for pattern recognition," *Opt. Letters*, pp. 1186-1188, 1991.
- [47] Z. Chen, Y. Zhang and G. Mu, "Complementary-reference joint transform correlator," *Appl Opt*, Vol 33, pp.7622-7626, 1994.
- [48] P. Martinez, M. Tejera, C. Ferreira, D. Lefebvre and H. Arsenault, "Optical implementation of the weighted sliced orthogonal nonlinear generalized correlation for nonuniform illumination conditions," *Appl Opt*, Vol 41, pp.6867-6874, 2002.
- [49] S. Zhang and M.A. Karim, "Morphologically preprocessed joint transform correlation", *Appl Opt*, Vol 38, pp. 2182-2188, 1999.
- [50] S. Zhang and M.A. Karim, "Illumination invariant pattern recognition with joint transform correlator based morphological correlation," *Appl Opt*, volume 38, pp.7228-7237, 1999.

